Brittle/Ductile and Plastic/Cataclastic Transitions in Experimentally Deformed and Metamorphosed Amphibolite

BRADLEY R. HACKER[1] AND JOHN M. CHRISTIE

Department of Earth and Space Sciences, University of California Los Angeles, California, 90024-1567

Abstract. The rheologies and deformation mechanisms of natural and hot-pressed synthetic amphibolite have been investigated at 0.5-1.5 GPa confining pressure, 650-950°C, and 10^{-4}-10^{-7} s^{-1} strain rate in Griggs-Blacic solid medium apparatus. The natural amphibolite failed and then slid stably along sample-scale fault zones at every pressure, temperature, and strain rate investigated. In contrast, the synthetic samples deformed along sample-scale fault zones only at fast strain rates and low temperatures, and were ductile at slower strain rates and higher temperatures. This ductility was apparently caused by defects introduced throughout the synthetic samples during the hot pressing. The fault zones in the natural rock exhibited a transition from crystal-plastic to cataclastic deformation coincident with the onset of melting. Fault zones developed at subsolidus conditions contain plastically deformed crystals, whereas fault zones developed at hypersolidus conditions contain glass and cataclastically deformed crystals.

INTRODUCTION

Although rocks of basaltic composition are common in oceanic crust and lower continental crust, their mechanical properties are poorly understood because experimentalists have devoted most of their efforts toward investigating peridotite, marble, and quartzite. Basaltic rocks vary systematically in their phase proportions and compositions (solid, liquid, and vapor) with pressure and temperature, and consequently, their mechanical behavior should change with conditions of metamorphism. Enhanced deformability during phase transformations may be significant in basaltic metamorphic rocks [*Brodie and Rutter*, 1985], just as phase transformations in gypsum [*Heard and Rubey*, 1966; *Murrell and Ismail*, 1976], serpentinite [*Raleigh and Paterson*, 1965; *Riecker and Rooney*, 1966; *Murrell and Ismail*, 1976; *Rutter and Brodie*, 1988], and chloritite [*Murrell and Ismail*, 1976] have profound effects on the nature and extent of their deformability.

This paper presents mechanical and microstructural data collected during an experimental investigation of the deformation and metamorphism of natural and synthetic amphibole-plagioclase rocks; the metamorphic changes are described in another paper. One objective of the study was to investigate the brittle/ductile transition in a relatively fine-grained (≈300 μm) natural amphibolite, but the rock was brittle over the whole range of accessible experimental conditions. A finer grained synthetic amphibolite (75-100 μm), formed by hot pressing powder of the same material, was deformed over the same range of conditions and exhibited a brittle/ductile transition. In this paper, "brittle" and "ductile" refer to macroscopic deformation style—whether the deformation is spatially concentrated or homogeneous, and "cataclasis" and "plasticity" are grain-scale deformation mechanisms referring to cracking and sliding or the movement of dislocations, respectively.

SLIP AND TWINNING MECHANISMS IN AMPHIBOLE AND PLAGIOCLASE

Amphibole

Amphiboles have very restricted slip and twinning systems. The observed mechanical twinning systems in clinoamphibole are (a) $K_1=(\bar{1}01)$, $\eta_1=[\bar{1}0\bar{1}]$; $K_2=(100)$, $\eta_2=[00\bar{1}]$; and (b) $K_1=(100)$, $\eta_1=[00\bar{1}]$; and $K_2=(\bar{1}01)$, $\eta_2=[\bar{1}0\bar{1}]$ [*Kirby and Christie*, 1977] referred to the conventional C2/*m* setting. The composition planes are $(\bar{1}01)$ and (100), hence the twins are reciprocal. By analogy with clinopyroxene, both types of twin should form by movement of $\frac{1}{2}[00\bar{1}]$ partial dislocations in (100) octahedral layers. The propagation of (100) twins should occur by the glide of partial dislocations in a manner analogous to the glide of unit dislocations to produce simple shear of a single

[1] Now at Department of Geology, Stanford University, California 94305-2115.

crystal. The propagation of $(\bar{1}01)$ twins should occur by shear, at a high angle to the composition plane, on the reciprocal twin plane K_2=(100) in the reciprocal glide direction $[00\bar{1}]$, in a manner analogous to the formation of kinks. The kinking mechanism that forms $(\bar{1}01)$ twins should be a more difficult process to activate than the direct glide mechanism that forms (100) twins, and $(\bar{1}01)$ twins should be rarer, wider, and require higher resolved shear stress for formation than (100) twins [*Kirby and Christie*, 1977].

Experimentally deformed amphiboles, however, commonly contain $(\bar{1}01)$ twins, but lack (100) twins [*Buck and Paulitsch*, 1969; *Buck*, 1970; *Rooney et al.*, 1974; *Nielsen*, 1978]. *Dollinger and Blacic* [1975] suggested that $(\bar{1}01)$ twinning occurs in preference to (100) twinning because (100)[001] slip occurs at a lower critical resolved shear stress. *Burnley and Kirby* [1981] were able to produce (100) twins in experimentally deformed hornblende single crystals by deforming them with low resolved shear stress on the $(\bar{1}01)$ twin system, perhaps because the temperature was low, 600°C. Both (100) and $(\bar{1}01)$ deformation twins are found in naturally deformed rocks, although $(\bar{1}01)$ twins may be restricted rocks deformed under unusual conditions such as meteorite impacts and nuclear explosions [*Chao*, 1967; *Borg*, 1972; *Gavasci*, 1973; *Rooney et al.*, 1975; *Biermann*, 1981].

Based solely on the relation that dislocation energy is proportional to the square of the magnitude of the Burgers vector **b** [e.g., *Weertman and Weertman*, 1964], in amphibole **b**=[001] (5.3 Å) is more likely to operate than **b**=[100] (9.9 Å) or **b**=[010] (18 Å). Slip on (001) is unlikely because it would require breaking the amphibole I-beam chains. Slip along (100) is possible in the [001] direction, and perhaps even along [010] by slip of partial dislocations of Burgers vector $\frac{1}{x}$[010]. Slip along (010) is possible in the [001] direction, but unlikely in the [100] direction because the silicate tetrahedra would be forced to squeeze past one another. Thus, the most likely slip systems have **b**=[001], on all {hk0} planes, while (100)[010] or (010)[100] slip might occur in grains with high resolved shear stress (Table 1). Consequently, amphibole crystals should behave like a bundle of inextensible fibres, in the sense of *Cobbold and Gapais* [1986]. This fibrous "structure" does not allow elongation in directions normal or parallel to [001]; any elongation in these directions must involve [010] or [100] slip, twinning, cracking, etc.

Laboratory measurements of amphibole single crystals show considerable strength anisotropy. Compared to single crystals compressed parallel to [001], crystals compressed perpendicular to [001] are 15-20% weaker, crystals compressed at 20-30° to [001] are 50-80% weaker, and crystals compressed at 45° to [001] are 50% weaker (Figure 1) [*Rooney and Riecker*, 1973]. Deformation occurs by slip in all these orientations, except in crystals compressed parallel to [001], where $(\bar{1}01)$ twinning occurs.

TABLE 1. Potential Slip Systems in Amphibole

	[100]	[010]	[001]
(100)	X	Possible, but a unit Burgers vector would be 18 Å.	Easy slip system, with Burgers vector of 5 Å.
(010)	Requires tetrahedra to rub past one another.	X	Easy slip system, with Burgers vector of 5 Å.
(001)	Require I-beam chains to break.	Require I-beam chains to break; unit Burgers vector would be 18 Å.	X

"X" indicates combinations in which the potential slip direction does not lie in the slip plane.

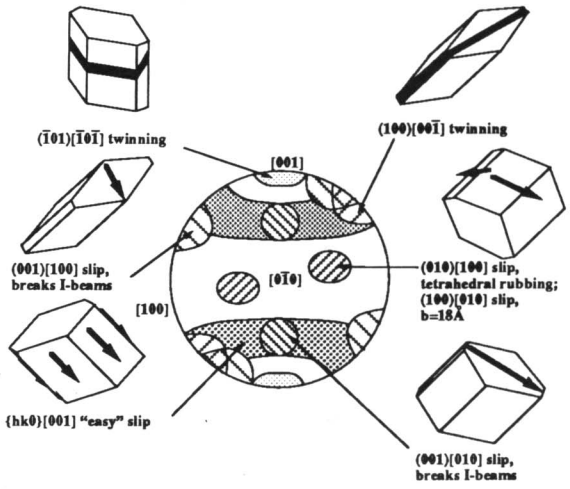

Fig. 1. Lower-hemisphere projection of a clinoamphibole crystal showing the compression directions that result in high resolved shear stress (≥0.75 of maximum shear stress) onto the reported slip and twinning systems. Note that the "easy" glide system cannot be activated by compression either parallel or perpendicular to the amphibole *c* axis [001].

Single crystals compressed parallel to (010) at 45° to [001] and in the acute angle between [100] and [001] form (100) twins and support greater stresses than crystals compressed in the obtuse angle between [100] and [001] [*Burnley and Kirby*, 1982]. This strength anisotropy of single amphibole crystals should impart a marked strength anisotropy to strongly lineated amphibole-bearing schists.

Deformation of hornblende single crystals at low temperatures (≤600°C) occurs by twinning and minor (010)[001], (010)[100] and (001)[100] slip [*Morrison-Smith*, 1976]. Amphibole polycrystals tested at temperatures of 600-750°C deform dominantly by (100)[001]

glide and by other unidentified slip systems at 800-950°C [*Dollinger and Blacic*, 1975; *Nielsen*, 1978]. One naturally deformed amphibolite examined by *Biermann and van Roermund* [1983] contains subgrains with {hk0} boundaries containing arrays of parallel [001] screw dislocations, and a few stacking faults parallel to (010) and bounded by $\frac{1}{x}$[001] partial dislocations. In summary, the clearly established plastic deformation mechanisms are slip on (100) and other {hk0} planes in the [001] direction; other slip directions in the {hk0} planes are less clearly established. The (100) and ($\bar{1}$01) twinning systems are activated only at high resolved shear stresses and provide only limited strains.

At high temperatures and slower strain rates within their stability fields, all amphiboles and amphibolites tested in the laboratory have been reported to deform ductilely [*Rooney and Riecker*, 1973; *Dollinger and Blacic*, 1975; *Nielsen*, 1978]. Amphibole is very strong when tested at low temperatures and pressures, but increased pressure [*Burnley and Kirby*, 1982; *Kirby*, 1987] or temperature [*Rooney and Riecker*, 1973; *Nielsen*, 1978] can lead to dramatic strength reductions by unknown mechanisms. For example, *Rooney and Riecker* [1973] reported strength differences of 50-90% over 200°C temperature intervals (near 800°C) in tests on single crystal and polycrystalline hornblende. *Rooney and Riecker* [1969; 1970; 1973; 1974; 1975] found that tremolite and hornblende single crystals and polycrystals were weaker at higher confining pressures (1.5 and 2.0 GPa) than at lower confining pressures (1.0 and 1.5 GPa). *Burnley and Kirby* [1982] also found similar strength reductions with increasing confining pressure in polycrystalline tremolite, and *Kirby* [1987] attributed this sudden weakening to tremolite breakdown. Marked weakening with increasing pressure is an unusual phenomenon and has been observed in amphibole, ice [*Kirby*, 1987], topaz [*Lee and Kirby*, 1984], epidote, tourmaline, and beryl [*Kirby and Lee*, 1982], and "wet" quartzite [*Blacic and Christie*, 1984].

Plagioclase

Numerous slip systems have been identified in plagioclase, but most of the dislocations are partials, which leave stacking faults on their slip planes. As a consequence, climb of these dislocations is very restricted because the stacking faults must migrate by diffusion as the dislocations climb. Thus recovery processes are slow, and strain hardening due to dislocation intersection and tangling is extensive.

There are two mechanical twin laws in plagioclase: 1) albite twinning, where the composition plane is (010) and the glide direction is the (non-rational) projection of the *b* axis on (010), and 2) pericline twinning, where the composition plane is the non-rational rhombic section and the glide direction is the *b* axis [*Tullis*, 1983, p. 313]. These twin systems are reciprocal, suggesting that both may form by slip of twinning partial dislocations in the (010) plane, by analogy with the amphibole reciprocal twinning mechanisms discussed above.

Plagioclase in the amphibolite deformed in this study has $C\bar{1}$ symmetry. Twinning in $C\bar{1}$ plagioclase is impossible at low temperature, but it becomes easier as the degree of ordering decreases (temperature increases) [*Brown and Macaudiere*, 1986]. $C\bar{1}$ plagioclases have only been twinned in experiments at 800°C and higher temperatures, where the plagioclase is in a high structural state [*Borg and Heard*, 1967, 1969, 1970; *Seifert and VerPloeg*, 1977]. However, plagioclase crystals of intermediate composition deformed naturally at temperatures considerably below 800°C contain mechanical twins [*Smith*, 1974; *White* 1975].

Based on the relation that dislocation energy is proportional to the square of the magnitude of the Burgers vector **b**, Burgers vectors on (010) in the $C\bar{1}$ structure should be $\mathbf{b}=\frac{1}{2}$[001], **b**=[100], or $\mathbf{b}=\frac{1}{2}$[201] [*Ji et al.*, 1988]. The prediction of slip on (010) in the *a* and *c* directions has been confirmed by TEM and preferred orientation studies by *Marshall and MacLaren* [1977a, 1977b], *Olsen and Kohlstedt* [1984, 1985], *Wenk et al.* [1986], *Montardi and Mainprice* [1987], *Ji et al.* [1988], and *Ji and Mainprice* [1988]. *Montardi and Mainprice* [1987] also identified defects belonging to the slip systems [100] (001), $\frac{1}{2}$[1$\bar{1}$1] (011) and [101] (10$\bar{1}$) in labradorite naturally deformed at amphibolite-facies conditions.

Microcracking is the dominant deformation mechanism in albite rock deformed at low temperatures (≤500°C in samples tested at 10^{-6} s^{-1} strain rate and 1.0-1.5 GPa) because thermally activated deformation mechanisms are difficult, and feldspar has excellent cleavages. At intermediate temperatures (500-650°C), cataclastic flow occurs by a combination of microcracking and slip; mixed cataclastic/plastic behavior occurs at 700-850°C. Because climb is difficult in albite, steady state dislocation creep at high temperatures (≥800°C) is accommodated by recrystallization and grain-boundary migration [*Tullis and Yund*, 1977, 1980, 1985, 1987]. Observations of naturally deformed plagioclase of intermediate composition indicate that microcracking is limited to temperatures ≤550°C [*Tullis*, 1983]. Intermediate composition plagioclases deformed at upper amphibolite- to granulite-facies conditions, where they were disordered, contain subgrains and recrystallized grains possibly formed by progressive subgrain rotation, implying easy recovery [*Vernon*, 1975; *Olsen and Kohlstedt*, 1985]. At lower amphibolite-facies conditions, where the plagioclase is ordered, recrystallization occurs by a nucleation mechanism, suggesting little or no recovery [*White*, 1975; *Borges and White*, 1980].

EXPERIMENTAL PROCEDURE

Starting Materials

Two starting materials were used: a natural rock and a synthetic rock. The natural rock is a strongly lineated and compositionally homogeneous amphibolite (specimen "TM-8") collected by us from the Klamath Mountains of northern

California, U.S.A.. It is composed of roughly 53% amphibole, 43% plagioclase, 2% ilmenite, 2% quartz, and trace amounts of rutile, sphene and apatite (Figure 2). The rock was selected for study because it has a granoblastic texture that permits easy determinations of experimentally produced changes in chemistry and texture.

The amphibole, a tschermakitic hornblende (classification of *Leake*, 1978), has the composition $K_{.05}\,Na_{.54}\,Ca_{1.6}\,Mg_{2.5}\,Mn_{.04}\,Fe_{1.8}\,Ti_{.11}\,Al_{.61}\,(Si_{6.3}\,Al_{1.7})\,(OH)_2$. It occurs as subhedral prisms with long dimensions (parallel to the crystal *c* axis) 0.6-1.2 mm, and short dimensions (perpendicular to *c*) 0.2-0.3 mm. Optically visible (100)[00$\bar{1}$] twins are rare, and cracks without measurable displacement occur along surfaces whose poles are inclined 0-20° to the *c* axis. The amphibole crystals contain a low density ($\approx 10^6$ cm^{-2}) of fairly straight dislocations; half are free unit dislocations and half occur in sub-boundaries (Figure 3). Stacking faults parallel to {110} are bounded by partial dislocations, suggesting that the crystals had deformed by {hk0}[001] slip of partial dislocations. The rock contains no other hydrous phases; hence an experiment conducted without added water can become hydrous only when the amphibole dehydrates (≥850°C at 1.0 GPa, and ≥750°C at 0.5 GPa).

The plagioclase is of composition An_{30} and occurs as anhedral equant crystals 0.2-0.3 mm in dimension. Few of the plagioclase crystals show undulatory extinction, but nearly all contain rare mechanical twins, rare stacking faults, low densities of partial dislocations ($\approx 10^6$ cm^{-2}), and the sub-microscopic (≈10 Å) phase modulation (e-type superstructure) that is common in intermediate plagioclases [*Nissen*, 1974; *Smith*, 1984] (Figure 3). Optically visible boundaries between adjacent plagioclase grains are planar or gently curved, and 120° grain-boundary triple junctions are common. Boundaries between adjacent plagioclase grains terminate against amphibole crystals at angles near 90°.

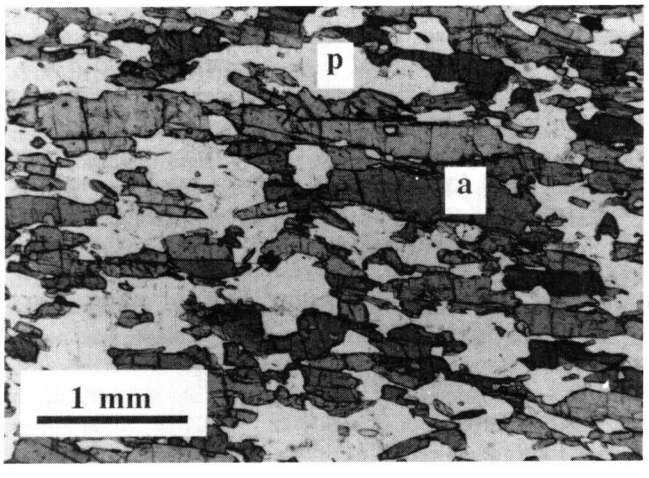

Fig. 2. Optical micrograph of the natural amphibolite starting material viewed perpendicular to the lineation. (**a**): amphibole; (**p**): plagioclase.

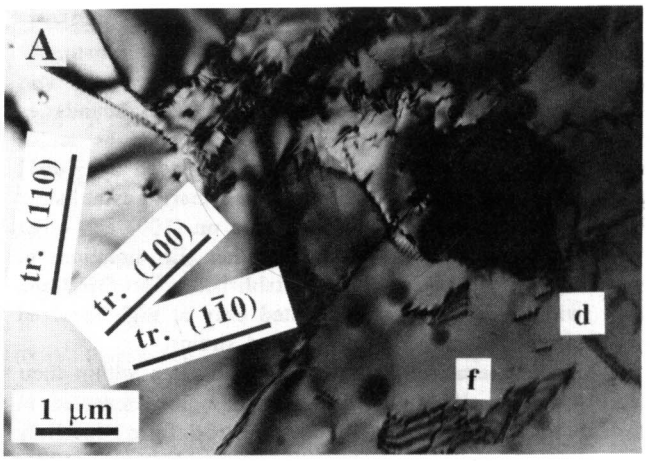

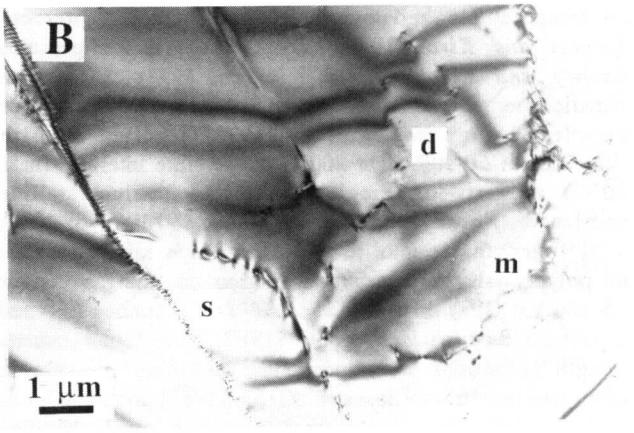

Fig. 3. Transmission-electron micrographs (TEM) of undeformed starting material. A: Amphibole crystal with stacking fault (**f**) planes parallel to the trace of (1$\bar{1}$0), and bounded by partial dislocations parallel to (110) and (100). Free dislocations (**d**) are parallel to (1$\bar{1}$0), (11$\bar{0}$) and (100). B: Plagioclase crystal with sub-boundaries (**s**), dislocations (**d**), and modulated structure (**m**). Diffraction patterns taken from areas of modulated structure contain two types of reflection from the C-centered lattice: *a* spots, and *e* spots produced by splitting of *b* spots.

The synthetic amphibolite was made by hot pressing a powder of the natural rock by a process described in detail below. Samples examined after hot pressing had no measurable porosity with either an optical or scanning electron microscope (Figure 4), but 0.1-0.5 μm pores at grain triple edges were seen by TEM (<1 vol%). Most of the rock was composed of heterogeneously deformed grains 75-100 μm in diameter; the remainder of the rock was made up of smaller highly deformed and locally recrystallized grains (as small as 1 μm) between the larger crystals. There was a slight tendency for the long axes of amphibole fragments to align perpendicular to the compression axis during the hot pressing. TEM of the hot-pressed aggregates before deformation showed that cores of large plagioclase grains contain twins and local dislocation tangles too dense to

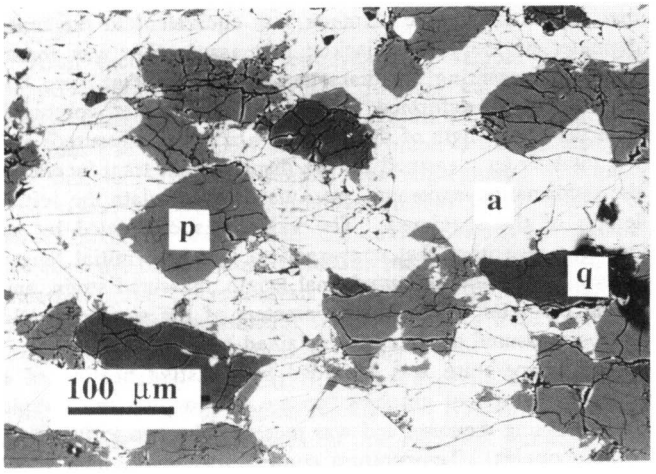

Fig. 4. BSEM of synthetic-amphibolite sample GB-1209 after hot pressing for 24 hours at 800°C and 1.0 GPa confining pressure. (a): amphibole; (p): plagioclase; (q): quartz. The obvious cracks formed during the decompression and cooling period at the end of the hot pressing.

count, or isolated curved dislocations (Figure 5A). Smaller plagioclase crystals were generally completely recrystallized. Amphibole crystals contained relatively straight dislocations in densities greater than those observed in the natural amphibolite (Figure 5B). Chemical analyses of hot pressed, but otherwise undeformed, synthetic amphibolite indicate that the compositions of the hornblende and plagioclase were relatively unchanged. No other phases, including quenched liquid, were observed in the hot-pressed specimens.

Experimental Apparatus

The experiments were conducted in piston-cylinder, solid-pressure-medium rock-deformation apparatus of the type designed by Griggs and coworkers [*Griggs*, 1967; *Blacic*, 1971]. The effect of water was investigated by adding 1 wt% water to some of the natural amphibolite samples. Every experiment on the synthetic amphibolite was done without adding water because the presence of water promotes development of porosity during hot pressing [*Luan et al.*, 1986]. Each experiment was taken to the desired pressure and temperature along a path such that the specific volume of free H_2O remained ≤ 1, and was then left undisturbed for ≈ 12 hours before the deformation began. The intrinsic oxygen fugacity of each experiment was determined by the rock, its jacket and confining medium, and was measured in two experiments by including small amounts of elemental and metal oxide powders. X-ray diffraction was used to determine whether the elemental and metal oxides were oxidized or reduced. In one run without added water at 950°C wüstite was oxidized and Ni remained reduced. In another run at 900°C with 1 wt% added water, Ni was oxidized and Cu remained reduced.

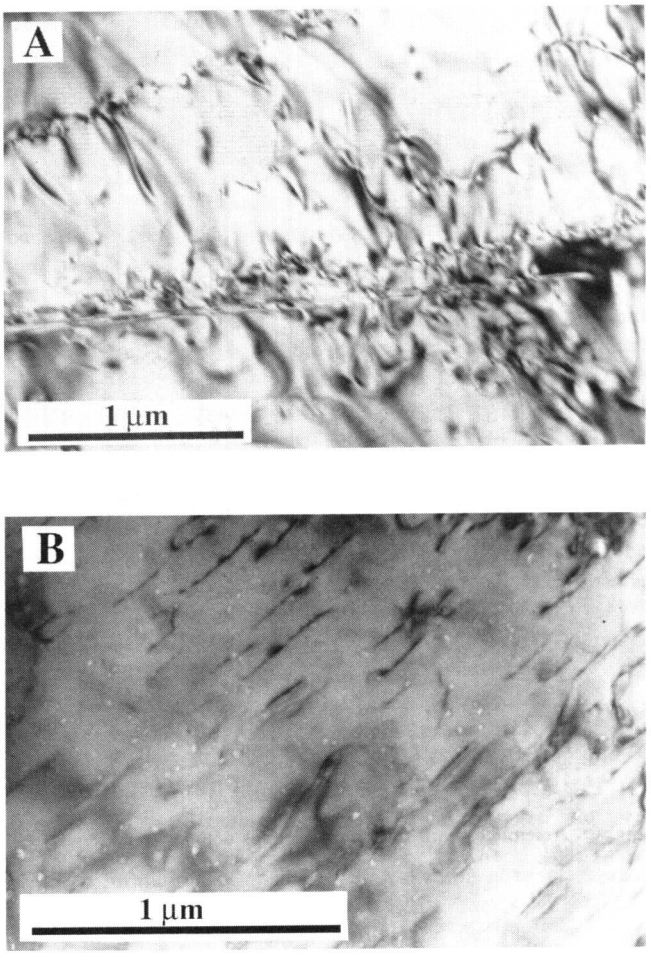

Fig. 5. TEM of synthetic amphibolite sample GB-1209 hot pressed for 24 hours at 800°C and 1.0 GPa confining pressure, showing moderate densities of defects relative to natural starting material. A: Plagioclase. B: Amphibole; spots are inferred to be associated with the dehydration of the amphibole.

The samples of the natural rock were right circular cylinders, 6.25 mm in diameter and 12.7 mm in length, cored with a water-cooled diamond drill. This sample size yielded approximately 25 grain diameters across the sample diameter. In experiments without added water, the sample was placed inside a ≈2 mm-thick copper cylinder confining medium. In experiments to which water was added, the sample was placed inside a 0.125 mm-thick cylindrical silver jacket surrounded by a confining medium of talc. The 1 wt% water was pipetted onto the top of the sample after the sample had been inserted into the silver jacket. The water was then "mechanically sealed" within the jacket by the two ceramic endpieces (Figure 6). The effectiveness of this seal is not quantitatively known, however, quartzose rocks tested in identical assemblies in our laboratory are damp at the end of experiments, indicating that some water remains in

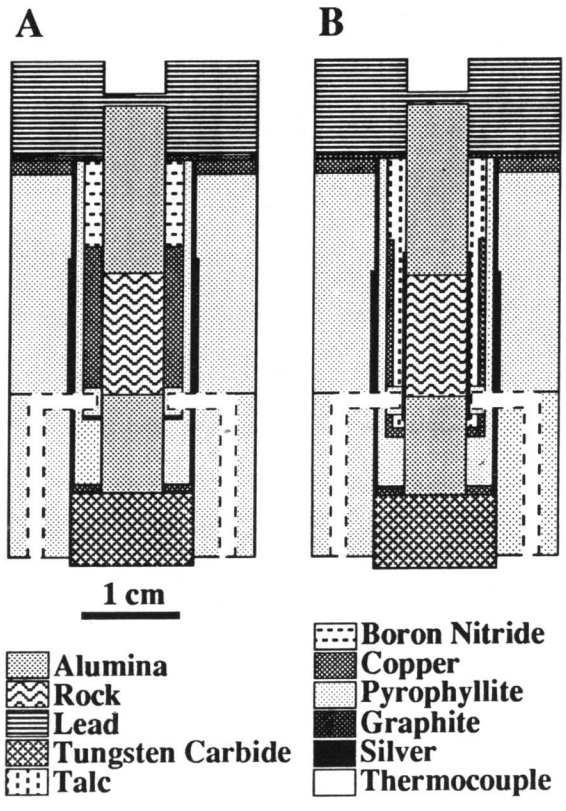

Fig. 6. Assemblies used to deform samples without (A) and with (B) added water.

contact with the sample during the experiments. The "wet" amphibolite samples were not damp at the end of the experiments, but they did show a measurable depression of the solidus relative to "dry" samples.

The powder for the synthetic amphibolite was prepared by grinding fragments of the natural amphibolite (TM-8) in tungsten carbide, and selecting the fraction with grain sizes of 75-100 μm. The powder was stored under vacuum at ≈75°C. Roughly 1 gram of the powdered amphibolite was poured into the copper jacket and shortened ≈75% with an Arbor press at room temperature; this yielded a sample ≈18 mm long and probably resulted in further cracking of grains. The confining pressure and temperature were then raised to 1.0 GPa and 500°C. The load and temperature were increased until a differential stress of 600 MPa and a temperature of 800°C were achieved. The sample was then heated for ≈12 hours, during which time the load relaxed to a value near the confining pressure. After the preheating period, the load piston was retracted from the sample endpiece an appropriate distance (≈0.04 mm), and the deformation experiment was begun at the adjusted temperature and pressure.

This hot-pressing technique did not allow direct measurement of the initial length and diameter of the synthetic rock. This limitation was overcome by assuming that the initial sample diameter was equivalent to the inner diameter of the copper jacket; this assumption was found valid by measuring the diameters of samples that were hot pressed but not deformed. This assumed diameter, combined with the final length of the sample (which was measured) and the total strain measured by the displacement transducers on the deformation apparatus, were used to calculate the initial length of the specimen. The value was calculated by an iterative algorithm that converged to a unique initial length determined by the measured final length, measured strain, and initial diameter. (The final diameters of the samples could not be measured directly, as explained below.)

The temperature was provided by resistive heating of a stepped cylindrical graphite furnace surrounding the sample and confining medium, and was measured by two $Pt/Pt_{90}Rh_{10}$ thermocouples. Temperature control was better than ±3°C precision for most experiments. Temperatures were not corrected for pressure or differential stress effects on the thermocouple e.m.f., which should result in an uncertainty of ±4.2-6°C for temperatures of 650-950°C at a confining pressure of 1.0 GPa [*Getting and Kennedy*, 1970; *Mao and Bell*, 1971]. The $Pt/Pt_{90}Rh_{10}$ thermocouples themselves are stated to measure temperatures accurately to ±3-5°C for temperatures of 650-950°C. The experiments were quenched rapidly: an experiment at 850°C cooled to 400°C in 10 seconds and 225°C in 20 seconds. The thermal profiles in the assemblies used in this study should be similar to those presented by *George and Christie* [1979], i.e., longitudinal temperature variations were <20°C and restricted to the end 10% of the sample length. The confining pressure measured was not corrected for friction within the assembly or the strength of the confining medium.

The output from the displacement transducers, force gauge, pressure gauge, and one thermocouple, was monitored by a Molytek datalogger/recorder. The datalogger/recorder printed all information on a strip chart, and transmitted it serially through a cable to a Macintosh microcomputer. The computer 1) received and deciphered the serial transmissions from the datalogger/recorder; 2) stored the transmitted data magnetically on disk; and 3) immediately calculated and displayed real-time stress-strain curves, allowing continuous evaluation of experiments in progress. After the completion of experiments, the data on disk were reanalyzed to allow more precise calculations. Strain and strain rates were calculated from the displacements measured by two displacement transducers, correcting for apparatus distortion and changes in sample diameter during deformation. Uncertainty introduced in the strain measurement by apparatus-distortion calibration and nonlinearity of the displacement transducers is estimated to be less than 0.5%. The differential stress was calculated as the difference between the axial stress and the confining pressure, and corrected for apparatus distortion and changes in sample diameter during deformation. The samples showed minimal barreling, causing uncertainties in the calculated strains and stresses of <5 and 10%, respectively.

Analytical Methods

After each experiment terminated, the sample jacket was removed incrementally with a tungsten carbide bit on a lathe. Chemical treatment to remove the jacket or confining medium was specifically avoided to preserve the chemistry of the sample. Then the sample was impregnated with resin and sawed in half. One doubly polished 30-μm section of every sample was made for examination by optical microscopy, back-scattered electron microscopy (BSEM), and electron-probe microanalysis (EPMA). Additional doubly polished <30 μm sections of selected samples were made and thin foils prepared for examination by TEM.

The chemistry and texture of the experimental products were investigated by optical microscopy, BSEM, EPMA, and TEM, to determine the physical and chemical processes that occurred during the experiments. Volume fractions of glass in samples were estimated from BSEM images; because of the difficulty in counting small glass fractions, samples noted to contain 1 vol% glass may actually contain between 0.1 and 2.0 vol%. Small-scale textural observations and chemical analyses of the phases were made with a four-spectrometer Cameca Camebax electron-probe microanalyser using well-characterized natural and synthetic mineral standards. A JEOL JEM 100-CX TEMSCAN microscope, equipped with a beryllium double-tilt goniometer stage, was used in the transmission mode to characterize the submicroscopic structure, and in the scanning/transmission electron microscopy (STEM) mode with a Kevex®-Ray 3203-100c-VS energy-dispersive X-ray detector connected to a Tracor™ Northern NS-880 analysis system for phase identification.

RESULTS

Experiments were conducted for periods of up to 649 hours at temperatures of 650-950°C, confining pressures of 0.5-1.5 GPa, and strain rates of 10^{-4}-10^{-7} s^{-1} (Tables 2 and 3; Figure 7). Metamorphic reactions occurred in all experiments at temperatures >650°C. Melting of amphibole + quartz + plagioclase occurred in all samples to which water was added. Dehydration melting of amphibole + quartz + plagioclase occurred at temperatures ≥850°C in samples deformed without added water. At ≥950°C and 1.0 GPa confining pressure, neoblasts of augite and hypersthene grew at the expense of amphibole and quartz. These chemical and mineralogical changes are described in another paper.

Our original objective to document the brittle/ductile transition in natural amphibolite under experimental conditions was unsuccessful. All our natural amphibolite samples, whether deformed with or without added water, deformed by faulting. The fault zones did show a clear transition from crystal-plastic to cataclastic deformation coincident with the onset of partial melting. Only by hot-pressing synthetic samples were we able to induce significant ductility in amphibolite.

Natural Amphibolite

Mechanical data. Samples of natural amphibolite invariably shortened by faulting, primarily along zones inclined ≈30° to the compression axis (Figure 8). It is certain that the faulting did not occur during the initial stages of the experiments when the samples were heated, pressurized, and initially contacted by the load piston, because samples that were only hydrostatically heated after that stage are not faulted. Evidence of minor plastic and cataclastic deformation (in the form of local twinning, bending of crystals, and cracking) was observed throughout each sample, but most of the deformation was concentrated along the fault zones. For this reason, the mechanical data on the natural amphibolite are presented as shear stress and shear displacement resolved onto a 30° inclined surface rather than as conventional stress-strain curves. The shear stress is the component of the differential compressive stress resolved onto the down-dip direction of the fault zone (i.e., $\tau = (\sigma_1-\sigma_3)\cos(30°)/2$). The shear displacement is the component of the piston displacement resolved onto the down-dip direction of the fault zone.

Samples deformed without added water contain ≈1 vol% liquid at 850°C, and ≈1 vol% liquid and 1 vol% pyroxene at 900°C. Axial differential stresses supported by these samples generally depend on temperature and displacement rate, ranging from ≈100 MPa at a temperature of 950°C and a strain rate of 10^{-6} s^{-1}, to >2230 MPa at 650°C and 10^{-6} s^{-1} (Figure 9). Stress-displacement curves are not as reproducible at faster displacement rates, as is typical of brittle deformation. Considerable weakening at displacement rates of 10^{-6} mm s^{-1} at 750°C and 10^{-5} mm s^{-1} at 850°C marks the onset of greater ductility, and the fault zones in these samples are wider than most. In a "stable-sliding" test, the stress should reach a constant value at a given constant displacement rate. The stress cannot be expected to remain invariant because the area of the plane along which faulting occurs in a sample 1) decreases with increasing displacement, and 2) increases as the normal to the fault rotates toward the compression axis because of distributed shortening of the sample and end effects. Most samples supported approximately constant stress after yielding. Sample yielding was not accompanied by sudden stress drops or audible noises. Stick-slip behavior was not observed, (although this may be because of the relatively "soft" nature of the testing machine [*Paterson*, 1978]).

Effect of water, confining pressure, and orientation. Samples deformed with 1 wt% added water contain ≈1 vol% liquid at 750 and 850°C, and 1-5 vol% liquid and 1-6 vol% pyroxene at 900°C. These "wet" samples were significantly weaker than samples deformed without added water at temperatures of 750 and 850°C (compare Figures 9 and 10). However, at 900°C, samples deformed with and without added water supported approximately the same level of stress at each displacement rate tested.

TABLE 2. Experimental Conditions and Results for Natural Amphibolite

T (°C)	ú (mm s^{-1})	P_c (GPa)	P (GPa)	Or	H_2O	Max Stress	S.s. Stress	Time (hour)	Fault Zone Type	Experiment Number	
650	1.1 x 10^{-4}	1.0	>1.76	=	0	>2231	n/a		plastic	1138a	
"	10^{-4}	1.0	>1.02	‖	0	poor T control		12	cataclastic	1166	
"	2.8 x 10^{-5}	1.1	1.78	‖	0	2099	2099	59	cataclastic	1139	
"	1.5 x 10^{-6}	1.1	1.49	‖	0	1180	1180	297	plastic	1217	
700	1.9 x 10^{-5}	1.0	1.57	=	0	820	1661	81	plastic	1138b	
750	1.7 x 10^{-3}	1.1	1.55	‖	0	1502	1475	21	plastic	1216	
"	2.1 x 10^{-3}	1.1	1.49	=	0	1300	1300	30	p. rim & c. core	1136c	
"	1.8 x 10^{-3}	1.0	1.47	‖	1	1339	1279	6	plastic	1193b	
"	1.2 x 10^{-3}	1.0	1.54	‖	0	1441	1464	20	plastic	1203b	
"	1.8 x 10^{-3}	1.0	1.57	‖	0	n/a	1550	20	plastic	1203c	
"	1.1 x 10^{-4}	1.1	1.42	=	0	1083	?	30	p. rim & c. core	1136b	
"	1.9 x 10^{-4}	1.0	1.61	‖	0	1850	1781	8	plastic	1162	
"	10^{-4}	1.1	>1.09	‖	0	motor failure		12	plastic	1163	
"	1.8 x 10^{-4}	1.1	1.59	‖	0	1450	1450	20	plastic	1173	
"	10^{-4}	1.4	>1.44	‖	0	motor failure		14	?	1185	
"	1.9 x 10^{-4}	1.0	1.35	‖	1	919	919		plastic	1193a	
"	1.8 x 10^{-4}	1.0	1.48	‖	0	1300	1279	20	plastic	1203a	
"	2.3 x 10^{-5}	1.1	1.18	=	0	427	360	30	p. rim & c. core	1136a	
"	2.8 x 10^{-5}	1.0	1.23	=	0	517	545	46	plastic	1146	
"	2.0 x 10^{-5}	1.0	1.50	‖	0	1413	1356	70	plastic	1175	◊1
"	1.9 x 10^{-5}	1.1	>1.71	‖	0	1900	n/a	69	plastic	1178a	◊1
"	2.0 x 10^{-5}	1.5	2.14	‖	0	1785	1785	50	plastic	1187	
"	1.9 x 10^{-5}	1.0	1.28	‖	1	751	700	45	p. & c.	1191	
"	10^{-5}	0.5	.74	‖	1	708	708	58	cataclastic	1205	◊2
"	1.8 x 10^{-6}	1.0	1.28	‖	0	721	721	388	distributed?	1160	◊2
"	1.9 x 10^{-6}	1.0	1.10	‖	1	189	189	611	p. & c.	1195	
"	1.8 x 10^{-6}	1.5	1.78	‖	0	790	790	351	p. & c.	1202	◊2
850	1.9 x 10^{-3}	1.0	1.27	=	0	836	822	48	cataclastic	1137c	
"	1.9 x 10^{-3}	1.1	1.42	‖	0	1037	1009	11	cataclastic	1164	*1
"	2.0 x 10^{-3}	1.0	1.33	=	0	945	889	19	p. rim & c. core	1189c	*1
"	1.8 x 10^{-3}	1.1	>1.12	‖	1	n/a	n/a	4	cataclastic	1190b	
"	1.8 x 10^{-3}	1.1	1.41	‖	0	1268	1055	20	cataclastic	1204b	
"	1.5 x 10^{-3}	1.1	1.48	‖	0	n/a	1254	20	cataclastic	1204c	
"	2.0 x 10^{-4}	1.0	1.16	=	0	527	494	48	cataclastic	1137b	
"	2.1 x 10^{-4}	1.0	1.34	‖	0	1007	965	17	cataclastic	1161	
"	2.0 x 10^{-4}	1.1	1.53	‖	0	1480	1351	69	plastic	1178c	*2
"	1.9 x 10^{-4}	1.0	1.26	=	0	769	686	19	p. rim & c. core	1189b	*2
"	1.9 x 10^{-4}	1.1	1.20	‖	1	254	236	4	cataclastic	1190a	
"	10^{-4}	1.0	>1.04	‖	1	poor T control		14	cataclastic	1196	
"	1.3 x 10^{-4}	1.1	<1.38	‖	0	1051	<965	20	cataclastic	1204a	
"	1.6 x 10^{-5}	1.0	1.08	=	0	273	231	48	cataclastic	1137a	
"	2.1 x 10^{-5}	1.0	1.15	=	0	506	430	56	cataclastic	1148	
"	10^{-5}	1.5	>1.53	‖	0	high friction		22	cataclastic	1176	
"	2.0 x 10^{-5}	1.1	1.30	‖	0	n/a	665	69	plastic	1178b	
"	2.0 x 10^{-5}	1.1	1.31	‖	0	640	640	50	p. rim & c. core	1186a	*3
"	1.9 x 10^{-5}	1.0	1.18	=	0	490	441	19	cataclastic	1189a	*3
"	1.8 x 10^{-5}	1.5	1.67	=	0	543	501	46	cataclastic	1188	
"	1.7 x 10^{-5}	1.1	1.16	‖	1	270	222	74	cataclastic	1197	
"	2.1 x 10^{-6}	1.0	>1.11	‖	0	279	>280	361	distributed?	1174	◊3
"	10^{-6}	1.5	>1.52	‖	0	high friction		96	plastic	1177	
"	1.9 x 10^{-6}	1.5	1.68	‖	0	501	501	579	cataclastic	1201	◊3
"	10^{-6}	0.5	>0.75	‖	1	747	n/a	93	p. & c.	1206	
900	1.9 x 10^{-3}	1.1	1.42	‖	0	1005	970	50	p. rim & c. core	1186d	
"	2.0 x 10^{-4}	1.1	1.30	‖	0	661	610	50	p. rim & c. core	1186c	
"	10^{-4}	1.1	>1.06	‖	1	n/a	n/a	20	cataclastic	1194	
"	2.1 x 10^{-5}	1.0	1.05	‖	0	115	115	43	cataclastic	1159	
"	1.9 x 10^{-5}	1.1	1.22	‖	0	n/a	351	50	p. rim & c. core	1186b	
"	1.8 x 10^{-5}	1.0	1.01	‖	1	21	9	69	cataclastic	1192a	
"	1.8 x 10^{-5}	1.0	1.13	‖	1	n/a	374	69	cataclastic	1192b	
950	1.7 x 10^{-5}	1.0	1.06	‖	0	115	115	36	p. rim & c. core	1157	

"ú": displacement rate parallel to fault zone; axial strain rate (s^{-1}) is 0.024 x displacement rate. "10^{-4}", "10^{-5}", and "10^{-6}" indicate experiments conducted at roughly $7.0x10^{-4}$, 10^{-5}, and 10^{-6} mm s^{-1} shear displacement rate on the fault zone; calculation of an exact displacement rate is not meaningful because the stress could not be accurately determined. "P_c": confining pressure. "P": mean normal stress. "Or": orientation of lineation with respect to compression axis; "=": lineation perpendicular to compression; "‖" lineation parallel to compression. "H_2O": wt% water added. "Max stress": maximum differential stress (σ_1-σ_3) supported (MPa). "S.s stress": steady state stress differential stress (σ_1-σ_3) supported (MPa). "Time": total duration of experiment. "Fault zone type": Textural type of dominant fault zone; "p": plastic; "c": cataclastic. "n/a": not applicable. "?": stress too small to measure. "*" Denotes pairs of samples deformed parallel and perpendicular to the lineation. "◊" Denotes pairs and trios of samples deformed at different pressures.

TABLE 3. Experimental Conditions and Results for Experiments on Synthetic Amphibolite

T (°C)	Strain Rate (s^{-1})	P_c (GPa)	P (GPa)	Stress MPa	Strain (%)	Time (hour)	Experiment Number
650	10^{-5}	1.0	1.38	1145	20	20	1229
"	1.7×10^{-6}	0.9	1.48	1623	21	32	1213
"	1.7×10^{-6}	1.0	1.49	1500	23	83	1255
"	1.9×10^{-7}	1.0	1.26	800	7	285	1257
750	10^{-4}	1.0	1.39	1170	19	28	1219
"	1.9×10^{-5}	1.0	1.43	1300	24	22	1222
"	1.7×10^{-5}	1.0	1.51	1550	25	65	1254b
"	2.4×10^{-6}	1.0	1.30	890	22	172	1210
"	1.5×10^{-6}	1.0	1.23	720	25	65	1254a
"	1.7×10^{-7}	1.0	1.13	390	16	441	1264
850	1.7×10^{-4}	1.0	1.32	910	25	17	1228
"	1.9×10^{-4}	1.0	1.43	1240	23	25	1256b
"	2.1×10^{-5}	1.0	1.27	740	23	25	1256a
"	2.3×10^{-5}	1.0	1.21	634	28	20	1220
"	1.9×10^{-6}	1.0	1.14	332	24	66	1225
"	1.9×10^{-6}	1.0	1.15	450	13	29	1253
950	1.9×10^{-4}	1.0	1.18	553	27	17	1223
"	2.4×10^{-5}	1.0	1.07	175	34	20	1221
"	2.3×10^{-5}	1.0	1.08	190	48	20	1272b
"	1.9×10^{-5}	1.0	1.06	150	13	12	1262
"	1.9×10^{-4}	1.0	1.17	450	48	20	1272a

"10^{-4}" and "10^{-5}" indicate experiments conducted at axial strain rates of approximately 1.7×10^{-4} s^{-1} and 1.7×10^{-5} s^{-1}; calculation of an exact strain rate is not meaningful because the samples contain faults. "P_c": confining pressure. "P": mean normal stress. "Stress": steady state differential stress (σ_1-σ_3) supported (MPa). "Strain": axial shortening. "Time": total duration of experiment.

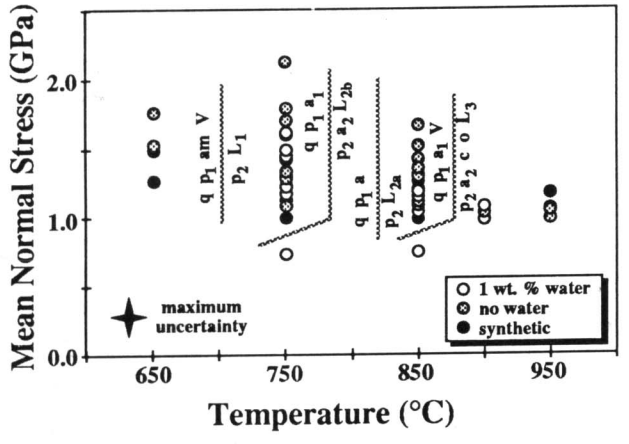

Fig. 7. Mean-normal-stress/temperature space showing pressures and temperatures of experiments conducted on natural and synthetic amphibolite and reaction boundaries. "a": amphibole; "p": plagioclase; "q": quartz; "c": clinopyroxene; "o": orthopyroxene; "L": liquid; "V": vapor.

Samples deformed at high confining pressure were all significantly stronger than samples deformed at lower confining pressures ("◊" symbols in Table 2). There were too few experiments at 0.5 and 1.5 GPa confining pressure to obtain a reliable determination of a frictional law of the form $\tau_s = \tau_o + \mu \sigma_n$, where τ_s is the shear stress and σ_n the

Fig. 8. Optical micrograph of natural amphibolite sample GB-1173 shortened 4.0 mm at 750°C, 10^{-5} s^{-1} strain rate, 1.11 GPa confining pressure, with no added water, at 1450 MPa steady state axial stress. The compression direction was parallel to the arrows.

normal stress on the fault; however, τ_o and μ estimated at 750°C and strain rates of 10^{-6} s^{-1} are 90 MPa and 0.34, respectively, and at 750°C and 10^{-7} s^{-1}, $\tau_o \approx 140$ MPa and $\mu \approx 0.12$.

Three 850°C tests on samples compressed perpendicular to the lineation may be compared with otherwise identical tests on samples compressed parallel to the lineation ("*" symbols in Table 2). Samples with the lineation perpendicular to the compression axis were weaker than those with the lineation parallel to the compression axis.

Microstructures. Deformation of the natural amphibolite samples occurred by microfaulting and intracrystalline slip primarily along fault zones inclined ≈30° to the compression axis. The fault zones approximate two half-cones that are concave toward the ends of the sample and join near the center. The samples initially have a 2:1 length to diameter ratio, so that a single fault initially inclined 30° to the cylinder axis becomes bent during shortening. Fault surfaces seen in thin sections cut roughly parallel to the fault surfaces vary from wavy to straight. Deformation is localized in the immediate vicinity of the fault zones. Many crystals in the bulk of deformed samples appear similar to the starting material in TEM; other crystals contain high densities of cracks, twins, tangled dislocations, or sub-micron-sized recrystallized or broken grains.

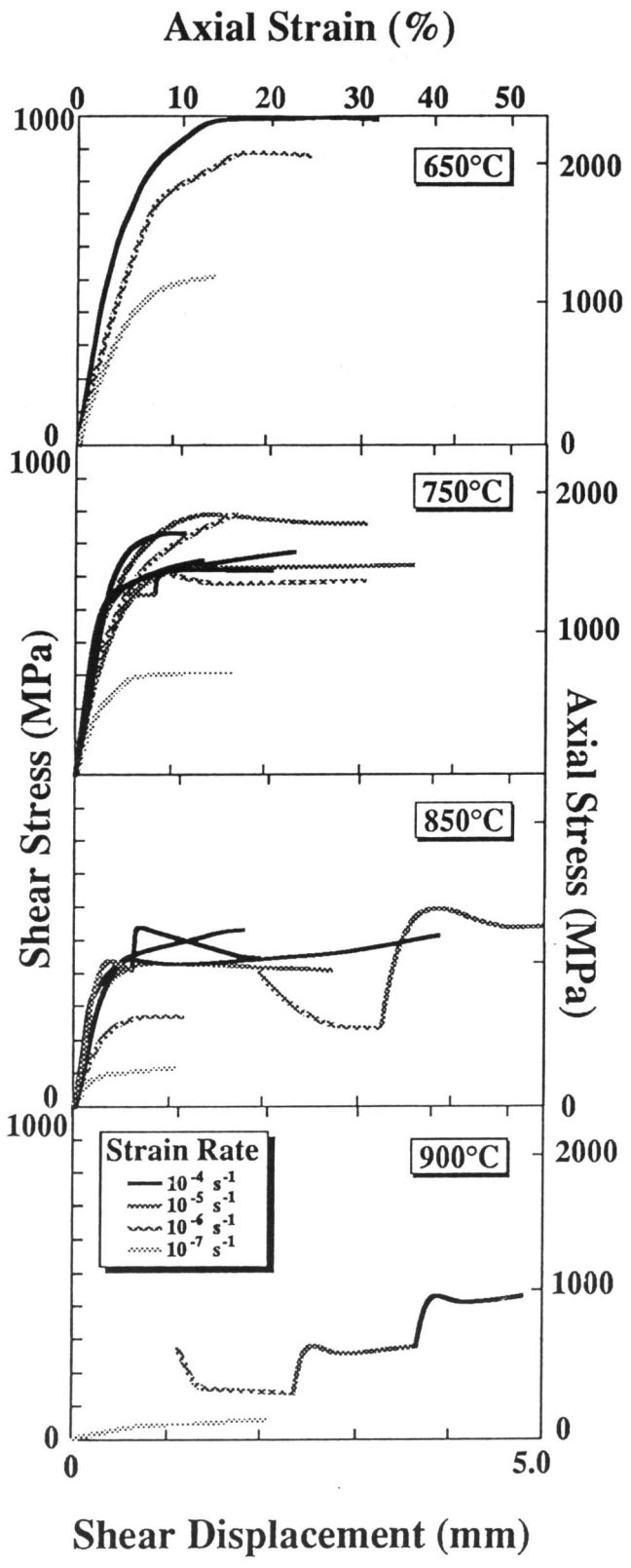

Fig. 9. Shear stress vs. shear displacement (resolved onto a fault zone inclined 30° to the compression axis) for tests conducted without added water at a confining pressure of 1.0 GPa, on natural amphibolite compressed parallel to its lineation. Equivalent axial differential stress and shortening strain are shown at right and top, respectively. The curves at 850°C and 900°C that begin abruptly at 10% and 5% strain are for samples initially deformed at 750°C and 850°C, respectively.

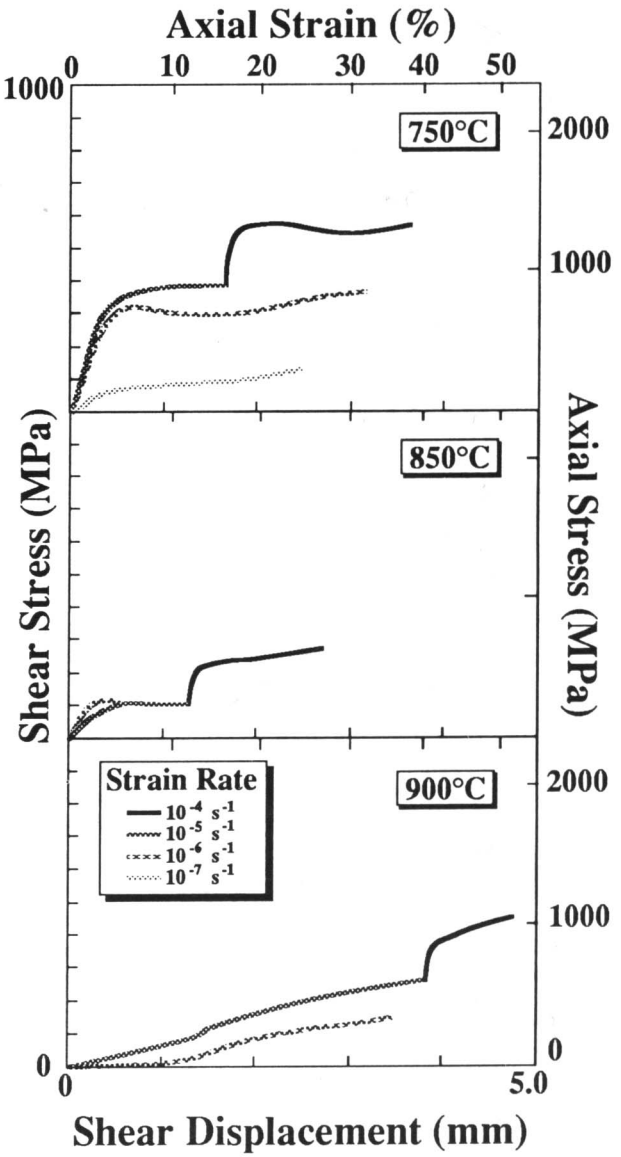

Fig. 10. Shear stress vs. shear displacement for tests conducted with 1 wt% added water at a confining pressure of 1.0 GPa, on natural amphibolite compressed parallel to its lineation. Equivalent axial differential stress and shortening strain are shown at right and top, respectively.

Fault zones commonly terminate at the edge of a sample, but some die out within the sample by branching into numerous narrow fault strands. Movement along subparallel strands resulted in pronounced deformation of crystals between the surfaces, and the fault surfaces either coalesce into one major fault or remain as a group of subparallel faults. These narrow strands terminate along grain boundaries or within crystals as optically visible deformation bands, undulatory extinction, or branching microcrack networks. Faults within crystals are visible in TEM as discrete cracks, or broader bands of very high dislocation density with local glassy patches and sub-micron scale crystal fragments (Figure 11).

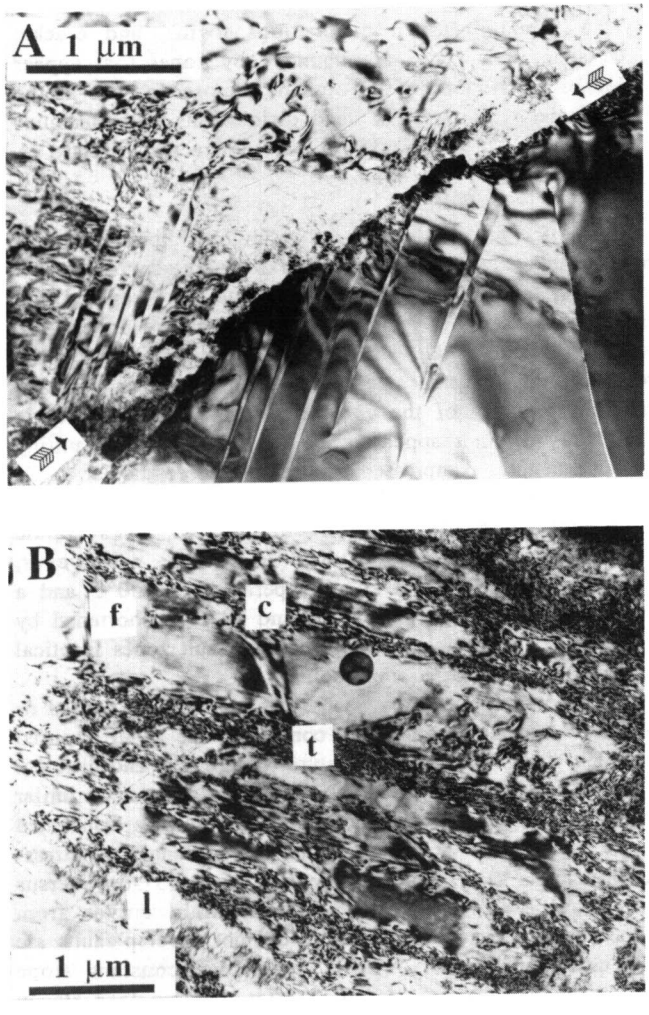

Fig. 11. TEM of plagioclase crystals in partially melted natural amphibolite sample GB-1148 shortened 3.7 mm at 850°C, 10^{-6} s^{-1} strain rate, 1.01 GPa confining pressure and 430 MPa steady state axial stress. A: Fault zone (arrows) with deformation twins and dislocations; glass within the fault zone is not visible at this magnification. B: Stacking faults (**f**), cracks (**c**), and twins (**t**) appear to have formed together. The slip zone (**l**) cuts across the other structures and consists of tangled dislocations.

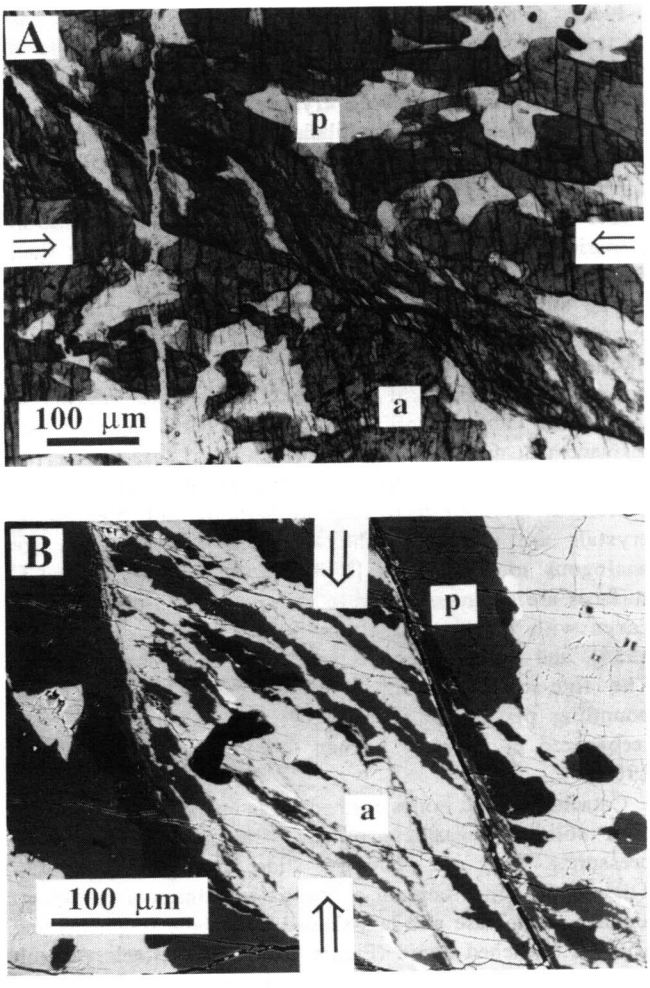

Fig. 12. A: Plane-polarized optical micrograph of a plastic fault zone in unmelted natural amphibolite sample GB-1162 shortened 3.5 mm at 750°C, 10^{-5} s^{-1} strain rate, 1.02 GPa confining pressure, with no added water, at 1781 MPa steady state axial stress. (**a**): amphibole; (**p**): plagioclase. The compression axis is shown by arrows. B: BSEM of plastic fault zone formed in unmelted natural amphibolite sample GB-1173 shortened 4.0 mm at 750°C, 10^{-5} s^{-1} strain rate, 1.11 GPa confining pressure, with no added water, at 1450 MPa steady state axial stress.

Two distinct types of fault zone are recognized: plastic fault zones and cataclastic fault zones. Plastic fault zones contain subparallel faults bounding plastically deformed amphibole and plagioclase crystals with a strong shape preferred orientation; they do not contain quenched liquid (Figure 12A). Plastic fault zones formed in samples deformed at subsolidus conditions, regardless of strain rate or confining pressure. They are ≤600 μm wide, averaging ≈135 μm. The crystals within plastic fault zones contain optically visible undulatory extinction and subgrains, and in TEM, microcracks, dislocation tangles, rare stacking faults, many twins, and some recrystallized grains are visible.

Plastic fault zones along which limited displacement has occurred contain crystals bent in "S" or "Z" shapes like a classic shear zone [e.g., *Ramsay and Graham*, 1970] (Figure 12B); individual amphibole crystals are bent as much as 110°. Curiously, bent amphibole crystals are never present on directly opposite sides of well-developed plastic fault zones. This may be because the initial fault zone was less planar than the well-developed fault zone, and the increase in planarity was effected by consumption of already bent (i.e., defect-laden) crystals on protruding portions of the fault.

The strong crystal shape preferred orientation and the subparallel fault surfaces of plastic fault zones are morphologically similar to the S and C (schistosité and cisaillement) surfaces of some natural tectonites [*Berthé et al.*, 1979]. The subparallel faults that bound the zones are displacement discontinuities analogous to C surfaces [*Berthé et al.*, 1979]; the surfaces defined by the strong shape preferred orientation of the amphibole and plagioclase crystals are related to the local finite strain, and are analogous to S surfaces [*Berthé et al.*, 1979]. S and C surfaces are commonly used to identify the sense of shear in zones with non-coaxial strain history [*Lister and Snoke*, 1984], and our experiments support such an interpretation. The fine-scale layering visible in some of the faults bounding plastic fault zones (Figure 12) has also been recognized in naturally formed C surfaces [*Vernon et al.*, 1983].

Cataclastic fault zones formed in samples deformed above their solidus, regardless of the strain rate or confining pressure. They are ≤600 μm wide, averaging ≈150 μm. These fault zones contain a breccia of micron-sized equant angular plagioclase and lath-shaped amphibole fragments and ≈5-10% quenched liquid (Figure 13). Some cataclastic fault zones exhibit a shape preferred orientation formed by the long axes of amphibole fragments parallel to the fault zone borders.

Incipient cataclastic fault zones with offsets of less than 1 μm follow grain boundaries or cut across crystals as 1) narrow bands of very high densities of dislocations or 2) arrays of en-echelon micro-faults that coalesce into a single fault on the opposite side of the crystal. Separate parts of crystals cut by incipient cataclastic fault zones commonly underwent different deformations (such as twinning in one half but not in the other). Samples tested with the lineation parallel to the compression axis typically contain only one cataclastic fault, but samples tested with the lineation normal to the compression axis contain numerous en-echelon cataclastic faults spaced 10-50 μm apart. In these samples, the sub-basal cracks in the amphibole crystals in the starting material are well oriented for sliding. Similar observations were made in a naturally deformed mylonitic amphibolite by *Allison and La Tour* [1977].

Amphibole crystals appear to control the textures of cataclastic fault zones—they protrude from fault-zone walls, and form asperities that ploughed through the fault gouge, creating local deformation gradients in the fault zone (Figure 14). These protruding amphibole crystals are themselves deformed only when they contact amphiboles protruding from the opposite wall. Cataclastic fault zones are often narrowest in areas where two amphibole crystals protruding from opposite walls of the zone are in proximity. Crystals adjacent to cataclastic fault zones are first deformed by dislocation glide and microcracking, then plucked from the fault zone wall, and finally comminuted further within the fault zone.

Deformation within cataclastic fault zones occurred by cataclasis and frictional sliding along intracrystalline surfaces and grain boundaries, most of which were wetted by silicate liquid. Plagioclase crystals contain mostly microcracks and tangled dislocations, although some isolated curved dislocations and twins are present. Amphibole crystals contain curved dislocations, twins, and cracks. Cataclastic fault zones are bounded by zones that appear finely recrystallized in the optical microscope, but at the TEM scale exhibit cracks and dislocations with densities too high to count (Figure 11) and are not recrystallized.

Synthetic Amphibolite

Mechanical data. Because the natural amphibole deformed by sample-scale faulting at all experimentally accessible pressures, temperatures, and strain rates, we prepared and tested a fine-grained synthetic amphibolite to investigate whether this unusual brittle behavior was caused by the relatively coarse grain size of the natural rock or by some inherent property of the constituent minerals. The fabric anisotropy did not appear to be the cause of the faulting because samples compressed parallel and perpendicular to the lineation both developed faults.

In contrast to the natural rock, most of the synthetic amphibolite samples shortened ductilely. However, synthetic samples tested at a temperature of 750°C and a strain rate of 10^{-4} s^{-1}, and 650°C and 10^{-5} s^{-1}, shortened by concentrated deformation along inclined fault zones identical to those in the natural amphibolite.

The stress supported by each synthetic sample, faulted or unfaulted, reached a relatively constant value at an imposed constant strain rate and temperature (Figure 15), and different samples tested under identical conditions supported similar stresses. Because of the ductility and uniformly distributed strain in the synthetic rock, the data are presented as stress-strain curves (i.e., axial differential stress, σ_1-σ_3, versus axial strain). Nearly all the stress/strain curves from experiments in which the samples did not develop faults are characterized by an "elastic" region of constant slope followed by a smooth transition after yielding to a steady state "flow" stress. The stress/strain curves for both experiments in which the samples faulted exhibit a maximum stress followed by a lower, steady state stress, similar to that observed in some natural amphibolite samples. In both experiments in which faults developed, the steady state stress was less than the steady state stress of unfaulted rocks deformed one order of magnitude more slowly at the same

temperature. This is particularly suprising because the effective strain rate in the faulted samples must have been even faster because the deformation was concentrated within a narrow zone.

A power-law fit of the relationship between steady state stress (MPa), strain rate (s^{-1}), and temperature (K) for the synthetic amphibolite tested at 650-850°C is $\dot{e} = 1.1\pm0.3 \times 10^{-4} \sigma^{3.7\pm0.3} \exp(-244\pm18/RT)$, where the activation enthalpy is in kJ $mole^{-1}$ (Figure 16). The values of steady state stress used in the regression fitting were taken from at least one single-strain-rate, single-temperature test for each temperature/strain-rate point. A second value

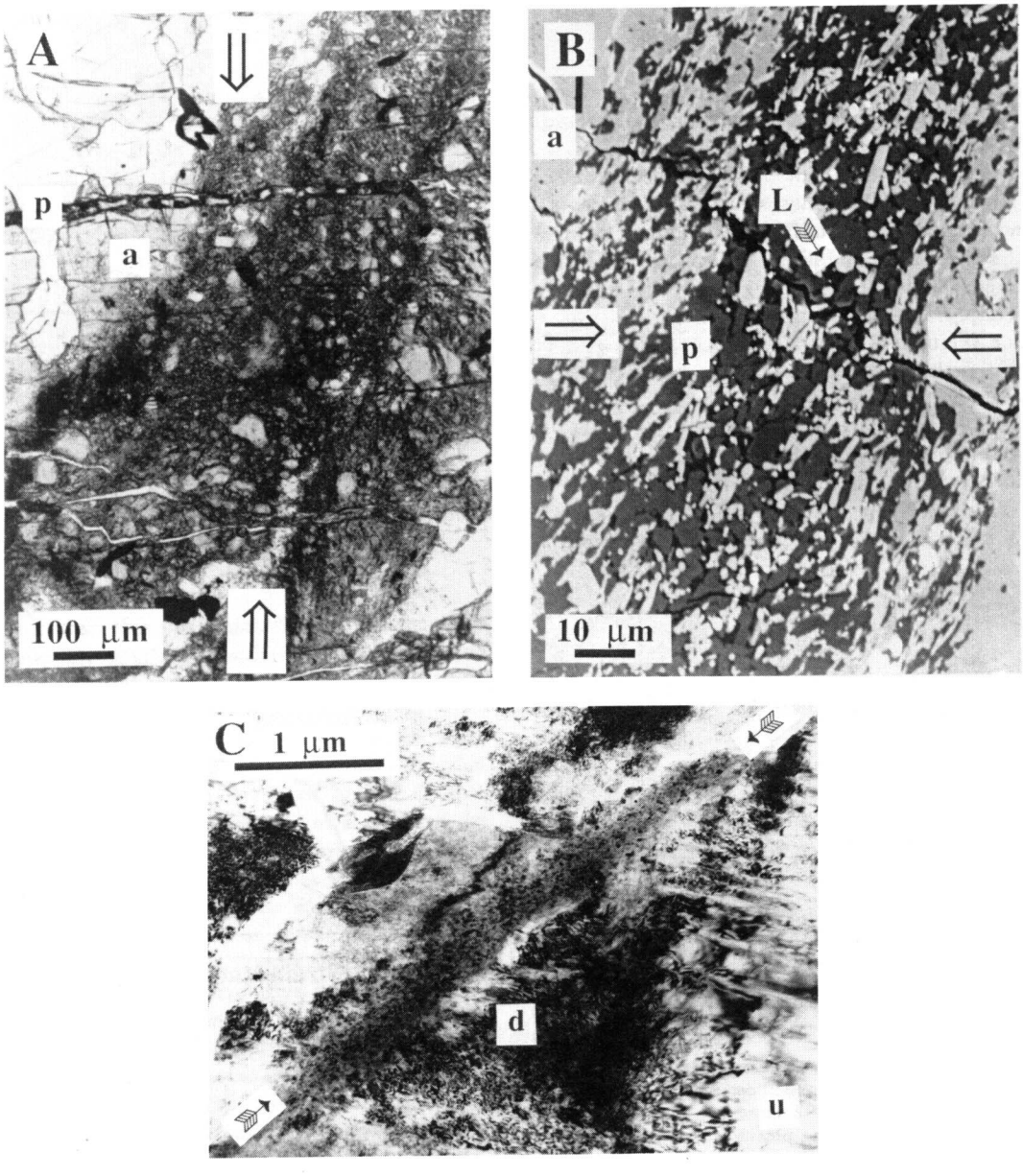

Fig. 13. Cataclastic fault zone formed in partially melted natural amphibolite sample GB-1157 shortened 2.1 mm at 950°C, 10^{-6} s^{-1} strain rate, 1.02 GPa confining pressure, with 1.0 wt% added water, at 115 MPa steady state axial stress. A: Plane-polarized optical micrograph; (a): amphibole; (p): plagioclase; compression axis is shown by arrows. B: BSEM illustrating that the deformation is cataclastic even at the scale of microns. (a): amphibole; (p): plagioclase; (L): glass (quenched liquid); the compression axis is shown by arrows. C: TEM of a plagioclase crystal in partially melted natural amphibolite sample GB-1148 that was shortened 3.7 mm at 850°C, 10^{-6} s^{-1} strain rate, 1.01 GPa confining pressure, with no added water, at 430 MPa steady state axial stress. The fault zone (arrows) is separated from the relatively undeformed part of the crystal (u) by a strongly deformed area (d).

for each strain rate of 10^{-4} to 10^{-6} s^{-1} was taken from a strain-rate stepping test. Measurements from samples tested at 950°C were fitted separately because these samples are anomalously weak and contain pyroxene formed at the expense of amphibole and quartz. A linear regression fit of the 950°C experiments yields $\dot{e} = 7.9 \pm 1.1 \times 10^{-10} \sigma^{2.0 \pm 0.3}$. Although the microstructures of the samples vary with temperature and strain rate, different constitutive relationships were not fitted to subsets of the data.

Microstructures. The synthetic starting material contained 75-100 μm grain cores with heterogeneously distributed twins and dislocations tangles separated by micron-sized recrystallized grains. With increasing temperature or decreasing strain rate, the microstructural features in amphibole and plagioclase crystals in the deformed samples evolve from sample-scale faulting, grain-scale cracking, twinning, and dislocation glide forming tangles, to subgrain formation (implying dislocation climb) and local recrystallization (Figures 17 and 18).

Sample scale faults occur at the fastest strain rates and lowest temperatures investigated. Intragranular grain-scale cracks are common in amphibole grains in samples tested at strain rates one order of magnitude slower than tests in which faulting occurs, specifically 850°C and 10^{-4} s^{-1}, 750°C and 10^{-5} s^{-1}, and 650°C and 10^{-6} s^{-1}; grain-scale cracks are much rarer in samples tested at strain rates two orders of

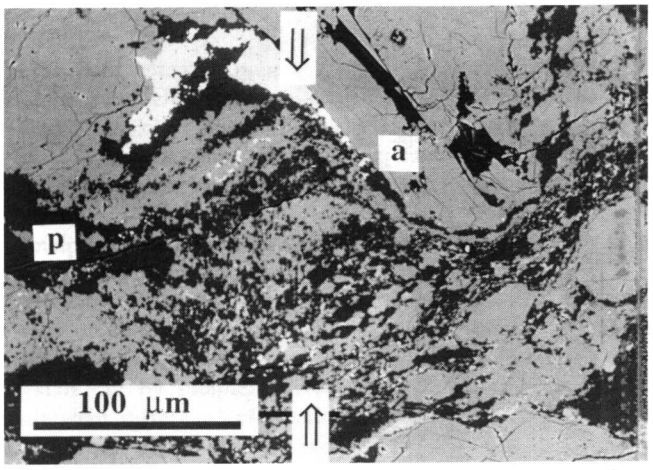

Fig. 14. BSEM of a protruding amphibole crystal (**a**) creating a local deformation gradient in a fault zone containing plagioclase (**p**) in natural amphibolite sample GB-1192 shortened 4.0 mm at 900°C, 10^{-6} s^{-1} strain rate, 1.01 GPa confining pressure, with 1.0 wt% added water, at 374 MPa steady state axial stress.

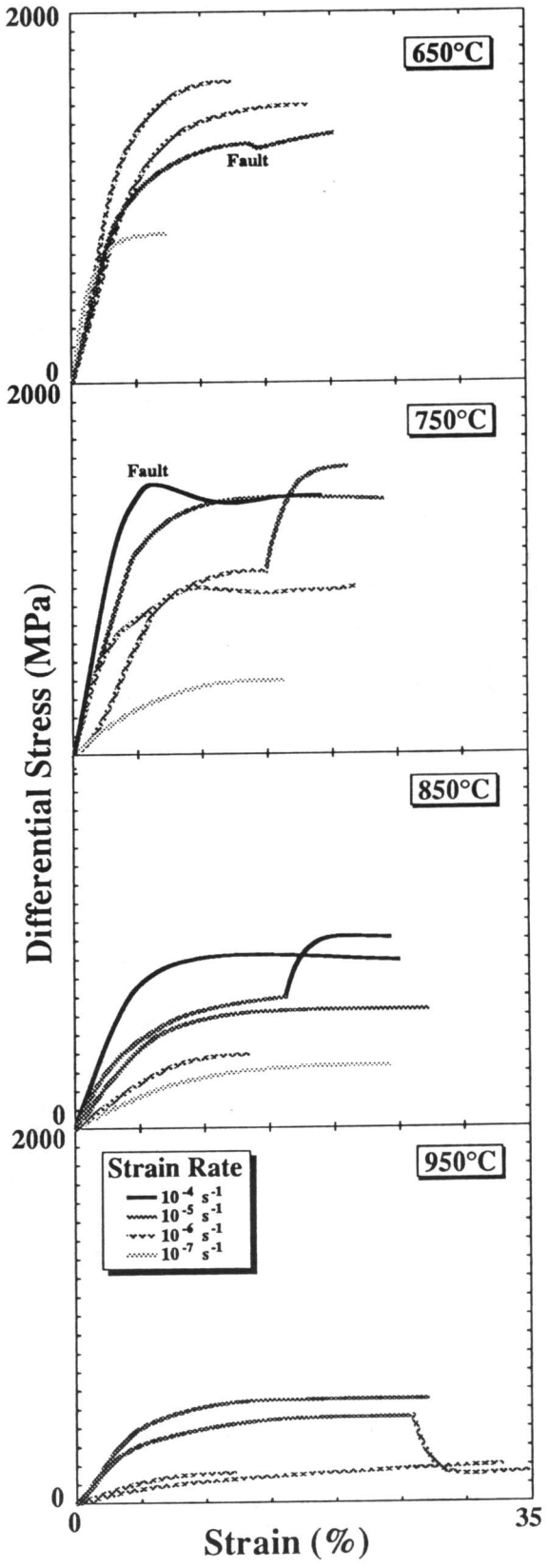

Fig. 15. Axial differential stress vs. axial strain for tests conducted on synthetic amphibolite at a confining pressure of 1.0 GPa. Samples that developed fault zones at 650°C, 10^{-5} s^{-1} and 750°C, 10^{-4} s^{-1} are labeled, and their mechanical data were not corrected for increase in sample diameter.

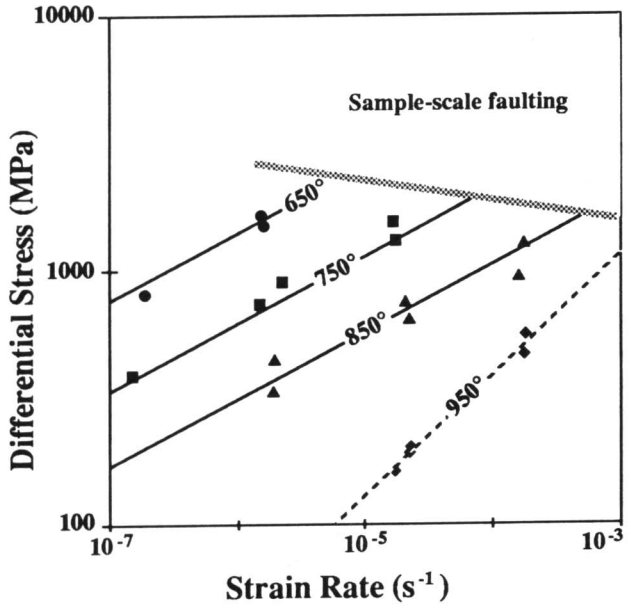

Fig. 16. Power law fit of the mechanical data collected for synthetic amphibolite. Samples that faulted at 650°C, 10^{-5} s^{-1} and 750°C, 10^{-4} s^{-1} are omitted from the multiple linear regression fit (full lines) of data at 650, 750, and 850°C. The 950°C data are incompatible with this fit and are fitted separately by linear regression (broken line); see text for fitted relation.

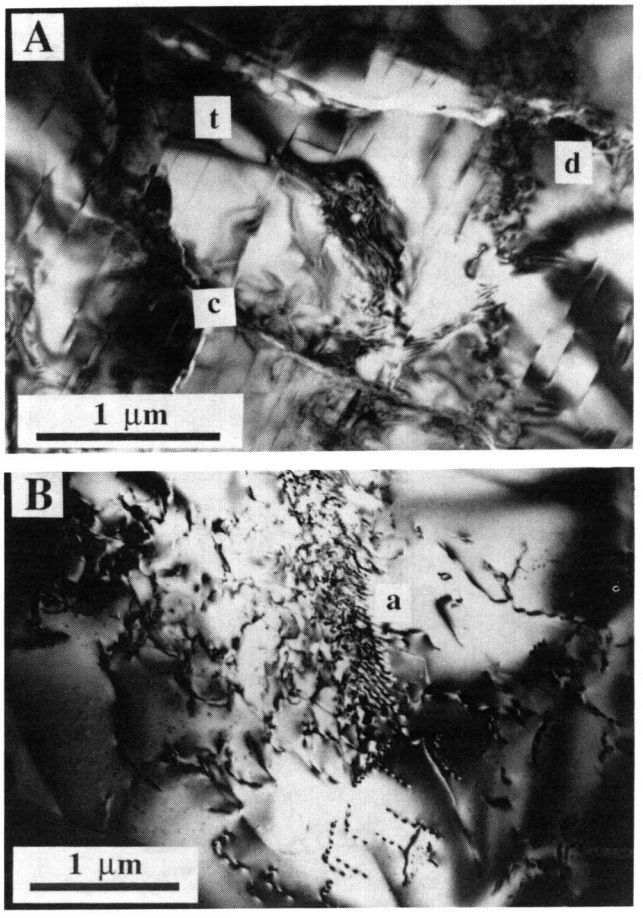

Fig. 17. TEM of unmelted synthetic amphibolite. A: Plagioclase crystal in sample GB-1229 strained 19% at 650°C, 10^{-5} s^{-1} strain rate and 1145 MPa flow stress, with dislocation tangles (**d**), cracks (**c**), and twins (**t**). B: Amphibole crystal in unmelted synthetic amphibolite sample GB-1257 strained 7% at 650°C, 10^{-7} s^{-1} strain rate and 800 MPa flow stress, with unit dislocations composed of straight segments with preferred crystallographic orientations. The dense array (**a**) of dislocations probably represents a dislocation pile-up.

magnitude slower than those in which faulting occurs. The cracks are commonly spatially associated with dislocation tangles, and some crack segments are parallel to twin boundaries.

Mechanical twins are present in plagioclase crystals deformed at all conditions; they are most common at strain rates of 10^{-5} and 10^{-4} s^{-1} or temperatures of ≥850°C (Figure 18A). Stacking faults, possibly developed as a result of the passage of twinning partial dislocations, are extensively developed in some plagioclase crystals under similar conditions. In amphibole grains, twins are uncommon and present only in samples deformed at faster strain rates or temperatures ≥850°C (Figure 18B). Twins and high densities of dislocations occur in mutually exclusive areas.

Dislocation glide formed tangles in plagioclase and amphibole at all conditions. Some of the tangles are wall-like and may form the kink and subgrain boundaries observed optically (Figure 17B). Free dislocations in plagioclase are generally straight at 650°C, and curved at higher temperatures. Evidence of climb in plagioclase, including strongly curved dislocations, loops, triple nodes, and recrystallized grains, is evident at 850°C. At similar temperatures, amphibole crystals contain subgrains (implying dislocation climb).

Amphibole crystals deformed at temperatures ≥750°C contain a number of features probably related to chemical breakdown of amphibole: 20-nm diameter tubes, pores, and small subhedral neoblasts of pyroxene. Some tubes serve as crack nucleation sites and others contain faceted neoblasts grown inward from the tube walls. The pores compose up to 2% of the crystal volume and are 20-60 nm in diameter [*Hacker and Christie*, 1988].

Discussion

Mechanical Anisotropy of Amphibole

Single amphibole crystals exhibit pronounced mechanical anisotropy, particularly with regard to the activation of possible slip and twinning systems. Compression parallel to the amphibole *c* axis produces large resolved shear stress only on the difficult $(\bar{1}01)$ twinning system, whereas

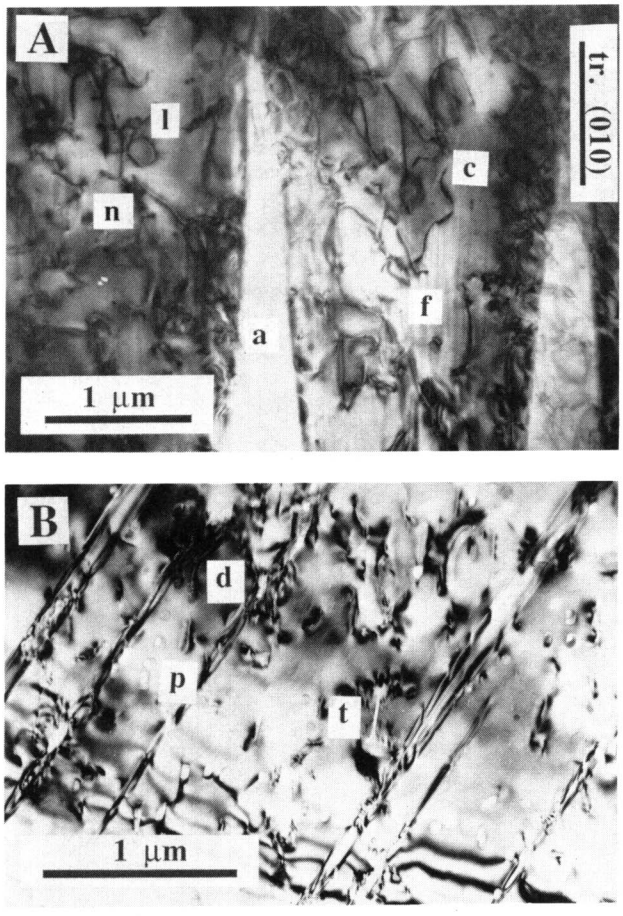

Fig. 18. TEM of crystals in partially melted synthetic amphibolite. A: Plagioclase crystal in sample GB-1253 strained 13% at 850°C, 10^{-6} s^{-1} strain rate and 450 MPa flow stress, with wedge-shaped albite deformation twins (**a**), curved dislocations (**c**) and loops (**l**). Stacking faults (**f**) parallel to (010) twin planes are extensively developed, possibly as a result of passage of twinning partials. The curved dislocations and triple nodes (**n**) indicate recovery. B: Amphibole crystal in synthetic amphibolite sample GB-1223 (strained 27% at 950°C, 10^{-4} s^{-1} strain rate and 555 MPa flow stress) contains stacking faults, twins, and relatively straight dislocations (**d**). Pores (**p**) and tubes (**t**) may have contained silicate-water fluid during the experiments and be associated with alteration of the amphibole.

compression perpendicular to the amphibole long axis produces high resolved shear stress on the (010)[100] and (100)[010] slip systems. Our observation that natural samples compressed parallel to the lineation at hypersolidus conditions are stronger than samples compressed perpendicular to the lineation, may be explained in part by the anisotropy of amphibole single crystals. The sample microstructures indicate that limited plasticity occurred prior to faulting; this may explain the differences in peak stresses supported by the rocks compressed in the two different lineation orientations. After failure, however, the deformation was accommodated within fault zones that lacked a lineation. Hence, the single crystal strength anisotropy can not be called upon to explain sample strength anisotropy after fault zone formation. Samples tested at hypersolidus conditions with the lineation parallel to the compression axis typically contain only one fault, but samples tested with the lineation normal to the compression axis contain numerous en-echelon cataclastic faults spaced 10-50 μm apart. In these samples, the sub-basal cracks in the amphibole crystals in the starting material are well oriented for sliding. We suggest that sliding along the sub-basal cracks combined with more distributed deformation in more numerous fault zones allowed the samples compressed perpendicular to the lineation to deform at lower stresses than the samples compressed parallel to the lineation.

The strength anisotropy of amphibolites should be a function of the amount of amphibole in the rock and the strength of the preferred orientation, and is probably most significant when amphibole forms the load-bearing framework of the rock. The rock strength anisotropy could change markedly as a result of reactions that produce or consume amphibole. Retrograde replacement of amphibole crystals by layer silicates such as biotite or chlorite might produce an even more mechanically anisotropic rock, because layer silicates have only one potential slip plane. On the other hand, prograde metamorphism of amphibolite could produce a much less mechanically anisotropic rock through the crystallization of pyroxene at the expense of amphibole. Specifically, the cell parameters a, c, and β in monoclinic pyroxene and amphibole unit cells are similar. The b cell dimension, however, doubles from ≈9 Å in pyroxene to ≈18 Å in amphibole. In pyroxene, slip in the [010] direction should be no more difficult than slip parallel to [100], whereas it is much more difficult in amphibole. In all inosilicates, slip on (001) is unlikely because it would require breaking silicate tetrahedral chains; hence, (100)[010] slip should be active in pyroxene. Reaction of amphibole to pyroxene should thus result in greater deformability and reduced mechanical anisotropy.

Brittle/Ductile and Plastic/Cataclastic Transitions

Our study of synthetic amphibolite confirms observations by previous investigators that deformation of amphiboles evolves from sample-scale faulting, grain-scale cracking, and twinning at low temperatures and fast strain rates to dislocation glide, dislocation climb, and recrystallization at high temperatures and slow strain rates. In contrast to previous studies on rocks containing 70-100 vol% amphibole [*Rooney and Riecker*, 1973; *Dollinger and Blacic*, 1975; *Nielsen*, 1978], however, our natural amphibolite, with ≈50 vol% amphibole, was brittle at all experimental conditions.

A brittle/ductile transition [*Heard*, 1960; *Griggs and Handin*, 1960] was observed with increasing temperature in

the synthetic amphibolite samples (all hot pressed and deformed without added water). At 650°C and $\dot{e} = 10^{-5}$ s^{-1} and at 750°C, 10^{-4} s^{-1}, the samples failed by faulting, as in the natural samples, but in all tests at higher temperatures and slower strain rates, the samples were ductile. Experiments by *Kronenberg and Shelton* [1980] at similar pressures indicate that diabase undergoes a brittle/ductile transition at similar temperatures and strain rates, although Kronenberg and Shelton's experiments are not directly comparable to ours because they investigated only one strain rate and used natural samples.

The experiments on the hot-pressed synthetic samples were designed (naively) to examine the effect of grain size on the mechanical properties of amphibolite. But it is probable that grain size is not the controlling factor in the transition to ductility observed in the synthetic aggregates, because the microstructure of the hot-pressed material is different from that of the parent natural amphibolite. Grain boundary regions of the hot-pressed amphibole and plagioclase grains examined by TEM were finely comminuted and plastically deformed, with local sub-micron-scale recrystallization in the strongly deformed portions. In these regions, a few residual ellipsoidal pores of sub-micron size were present, as in many sintered materials. We consider that the presence of abundant dislocations, twins, and stacking faults, and the stress concentrations associated with the pores, are responsible for nucleating additional defects and ultimately for the enhanced ductility of the synthetic amphibolite. Enhanced recovery and dynamic recrystallization caused by the greater concentration and variety of defects also contributed to the ductility. It is likely that the brittleness of the natural amphibolite is a result of its constituent minerals, amphibole and plagioclase, having limited plasticity, and few defects. That is, nucleation of twins and dislocations is difficult.

Marked strength reductions associated with samples deformed in talc at temperatures near 800°C observed by *Rooney and Riecker* [1973] and *Nielsen* [1978], were not found in the present study. Our jacketed "wet" samples deformed in talc confining medium are considerably weaker than "dry" samples deformed in copper, and we suggest that the strength reductions in earlier experiments were caused by talc dehydration and introduction of water into the sample.

Fault Zone Formation and Development

It is difficult to assess whether the fault zones were initiated within grains by a) brittle crack formation, b) crack propagation accommodated by plastic flow at crack tips, or c) local plastic deformation followed by fracture. The latter alternative, c) is supported by observations that amphibole and plagioclase crystals outside of fault zones did undergo limited plasticity, and that crystals adjacent to cataclastic fault zones first deformed by dislocation glide and microcracking before being plucked from the fault-zone walls. Limited dislocation glide and twinning in favorably oriented grains would have resulted in local strain and stress gradients, which in turn may have driven cracking. The paucity of slip systems in amphibole crystals also means that crystals oriented for {hk0}[001] "easy" glide systems can accommodate all shortening required in one region of a sample, thus localizing the deformation. This effect would be maximized in rocks containing large, similarly oriented grains.

Differences in thermal and elastic properties between plagioclase and amphibole and the elastic anisotropy of each phase may have contributed to the cracking. Principal values of the moduli, referred to conventional axes [*Birch*, 1966], indicate that the anisotropy of both minerals is large: maximum values of the principal Young's moduli of two hornblende crystals are larger than the minimum values by ≈70%; maximum values for two plagioclase crystals are larger than minimum values by 50-80%. On average, the two plagioclases are more compliant than the two hornblendes by ≈30% in compression and ≈55% in shear. If the maximum and minimum values do not coincide with the crystal reference axes, as is possible in crystals of low symmetry, these anisotropies must be minimal for each phase. Quartz, which is present in very small proportion in the rock, is even more compliant than plagioclase and will also cause local anisotropy of stress and elastic strain concentrations in its vicinity. Cracking probably was concentrated in the more compliant phases, generally plagioclase and possibly quartz. In the deformed natural amphibolite samples cracks are common and are associated with high dislocation and twin densities in the plagioclase, but intragranular cracks are relatively rare in the amphibole.

Once fault zones formed, they remained the loci of deformation. Many factors can weaken fault zones and ensure their preservation:

1) Reorientation of crystals may produce geometrical softening. This effect would be magnified in mechanically anisotropic crystals such as amphibole, where a single favorably oriented crystal can accommodate far more deformation than neighboring grains.

2) Reduced grain size (increased surface energy per unit volume) may promote the growth of new phases, leading to transformational weakening by providing small strain-free grains and local stress and elastic strain gradients caused by volume changes during chemical reaction.

3) Spatially concentrated microcracks or dislocations in fault zones could promote accelerated diffusion processes (*e.g.*, pipe diffusion) [*Hacker and Christie*, 1988].

4) Increased permeability in cataclastic fault zones could permit increased fluid flux and faster chemical reaction. Amphibole crystals have such a limited ability to deform by slip and twinning that fluid-induced microcracking could provide a necessary additional deformation mechanism. Effective normal stresses would also be reduced in the presence of liquid, promoting reduction in frictional resistance.

5) Chemical change can facilitate deformation by the processes described above, including vapor- or liquid-producing reactions, the growth of weaker solid phases, the breakdown of stronger phases, and other more unusual interactions. For example, the pores and tubes formed during the breakdown of amphibole [*Hacker and Christie*, 1988] served as nucleation sites for microcracks, providing an additional deformation mechanism not previously suspected to be available at high temperatures.

The first of these potential weakening mechanisms (1) can occur in any rock type, but the last four (2)-(5) are more likely to occur in polyphase rocks and are significant microstructural and microchemical interactions between deformation and metamorphism. All five are proven or suspected to have occurred during experimental deformation of amphibolite.

The microscopic deformation mechanisms within the amphibolite fault zones change from crystal plasticity to cataclasis, coincident with the transition from subsolidus to hypersolidus conditions. Plastic fault zones presumably formed because stresses were great enough to induce crystal plasticity and the effective pressure was great enough to suppress cataclasis. Cataclastic fault zones presumably formed because small amounts of silicate liquid present reduced the effective pressure and normal stress on the fault zone.

Naturally deformed amphibolites contain fault zones similar to those produced in this study. Current data do not allow inference of the conditions under which such natural fault zones are formed. Additional experiments could, however, be designed to define a more complete temperature/strain-rate relationship for the brittle to ductile transition, once the effect of the microstructures produced during hot pressing is understood. Perhaps the brittle/ductile transition in naturally deformed basaltic rocks could then be evaluated quantitatively.

Distribution of Liquid

The fault zones in the hypersolidus amphibolite samples contain ≈5-10 vol% liquid, whereas the rock outside the fault zones contains only ≈1 vol% liquid localized at amphibole-plagioclase-quartz triple junctions. The greater volume fraction of liquid in fault zones must have been generated locally, however, and could not have migrated from surrounding regions. The pools of liquid outside the fault zones are restricted to grain junctions of plagioclase, amphibole, and quartz grains; the quartz grains are separated from one another by several tens of microns, so that the liquid pools are unlikely to be interconnected. Only liquid that formed very near an incipient fault zone could have been incorporated into the zone. Comminution within the fault zone probably lead to production of additional liquid, both through increased surface area (i.e., increased surface energy per unit volume) and the increased likelihood of reactant phases being in contact or in chemical communication with one another. Dilatation during cataclasis might also have lead to local effective pressure drops that could cause melting.

Differential stress did not affect the liquid distribution within the unfaulted regions of the samples. As in hydrostatic experiments, the liquid remained in its source regions and did not segregate into grain boundaries or tubes. This is in harmony with observations of partially melted synthetic feldspar-quartz aggregates with 1-5 vol% liquid [*Dell'Angelo et al.*, 1987; *Dell'Angelo and Tullis*, 1988]. In the partially melted amphibolite with ≈1 vol% liquid, dislocation creep remained the dominant deformation mechanism, as in natural aplite with 5-10% liquid deformed under similar conditions [*Dell'Angelo and Tullis*, 1988].

Mechanical Data on Synthetic Amphibolite

The activation enthalpy determined for creep of the synthetic amphibolite (244±18 kJ $mole^{-1}$) is slightly less than the activation enthalpy reported for diabase (260-276 kJ $mole^{-1}$; *Shelton and Tullis*, 1981; *Caristan*, 1982], similar to that of anorthosite (234-238 kJ $mole^{-1}$; *Shelton and Tullis*, 1981], and significantly less than the activation enthalpy reported for creep of clinopyroxenite (335-380 kJ $mole^{-1}$; *Shelton and Tullis*, 1981; *Kirby and Kronenberg* 1984].

The stress supported by amphibolite can be compared to the strengths of other experimentally deformed rocks in the experimental range. A convenient way to illustrate this is to compare the flow stresses for a single temperature. Figure 19A shows the results of such a calculation for strain rates in the experimental range at 900°C. At laboratory temperatures and strain rates, the strength of synthetic amphibolite is roughly comparable to the strengths of diabase, anorthosite, albite rock, *Shelton and Tullis'* [1981] diopside rock, and *Koch's* [1983] "dry" quartzite.

It is dangerous to extrapolate the constitutive equations of polyphase aggregates, especially those containing even small volumes of liquid, far beyond the limits of the experimental range. Different phases have different flow laws, and experimental and theoretical analyses (e.g., *Jordan*, 1987) indicate that the mechanical behavior of a polyphase aggregate is not a simple function of the flow laws for the individual phases and the amounts of the individual phases. The presence of a fluid can also affect rheological properties. In spite of these caveats, extrapolation of the constitutive relations suggest qualitatively that amphibolites deform at stresses intermediate between those of the quartzose and ultramafic rock types, and comparable with those for other feldspar-bearing rocks. At a temperature of 500°C and strain rates of 10^{-10}-10^{-15} s^{-1}, amphibolite, diabase, albite rock, and anorthite rock should all flow at roughly similar stresses (Figure 19B). All four of these rock types should support roughly one order of magnitude greater stress than "wet" or "dry" quartzite and roughly two orders of magnitude lower stress than "wet" dunite and diopside rock.

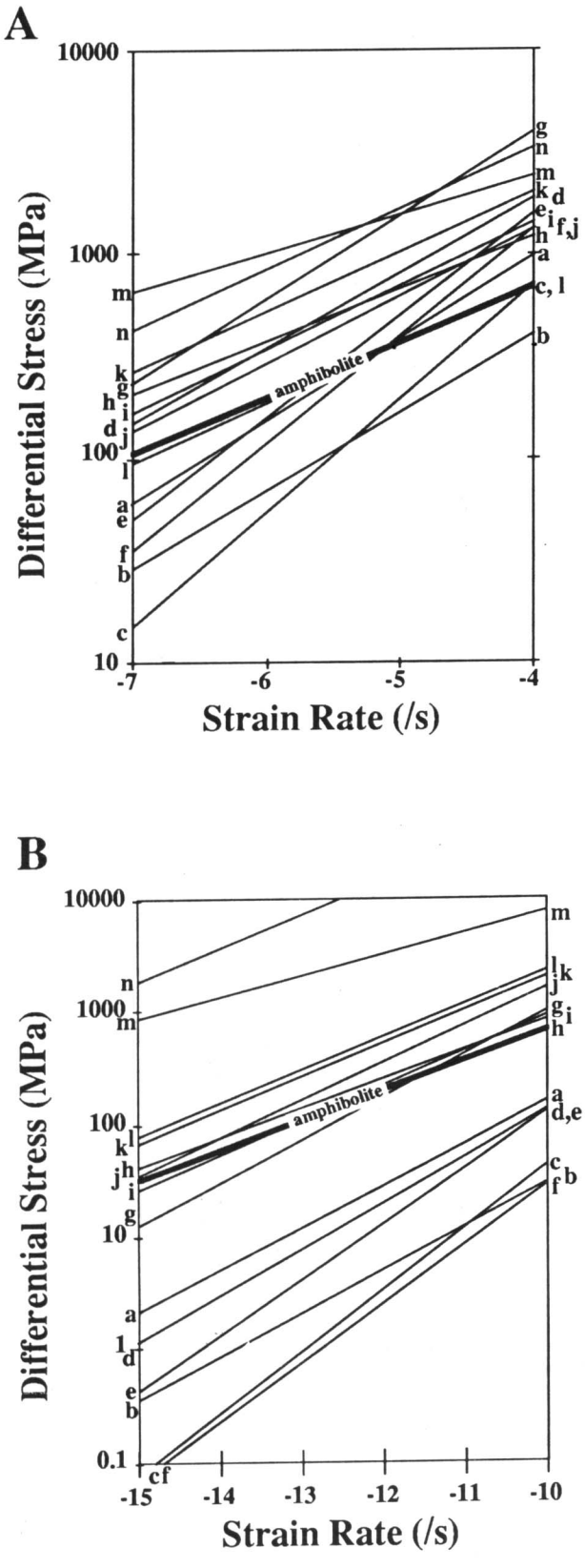

CONCLUSIONS

This study was exploratory, to investigate the transition from brittleness to ductility in amphibolite. Ductility was not attained in the natural rock over the accessible range of experimental conditions, and deformation was localized along narrow fault zones in all samples. Fault zones formed below the solidus contain predominantly plastically deformed crystals, whereas those formed above the solidus contain cataclastically deformed fragments with less evidence of plasticity.

The natural amphibolite was quite strong; samples tested without added water at 650°C supported differential stresses of >2.3 GPa. Samples tested with 1 wt% added water were systematically weaker (by 20-70%) than samples deformed without added water under otherwise identical conditions. Samples tested at high confining pressure were all significantly stronger than samples tested at lower confining pressure. Samples compressed perpendicular to their lineation were weaker than those compressed parallel to the lineation.

Most of the synthetic amphibolite samples shortened ductilely. This ductility was probably caused by the motion and recovery of defects introduced throughout the synthetic sample during the hot pressing, and by local recrystallization. However, samples tested at low temperatures and fast strain rates shortened by concentrated deformation along fault zones identical to those formed in the natural amphibolite. A brittle/ductile transitions of this type was first documented experimentally by *Hugh Heard* [1960] in limestones. The brittle/ductile transition in synthetic amphibolite may be a result of the smaller grain size of the synthetic rock relative to the natural rock, or an inherent property of amphibolite.

Acknowledgements. We thank N.L. Carter, A.K. Kronenberg and J. Tullis for their helpful reviews. This work was funded by NSF Grant EAR84-16781 (to J.M.C.) and a Sigma Xi research grant (to B.R.H.).

Fig. 19. A: Flow stresses for various rocks at laboratory strain rates and a temperature of 900°C. 900°C is outside the temperature range of the original experiments for some of these rock types. B: Flow stresses for various rocks extrapolated to a temperature of 500°C and geologic strain rates. a: "wet" quartzite [*Koch*, 1983]; b: "wet" quartzite [*Kronenberg and Tullis*, 1984]; c: "wet" quartzite [*Hansen and Carter*, 1982]; d: "dry" quartzite [*Koch*, 1983]; e: "dry" quartzite [*Shelton and Tullis*, 1981]; f: "dry" quartzite [*Hansen and Carter*, 1982]; g: quartz diorite [*Hansen and Carter*, 1982]; h: albite rock [*Shelton and Tullis*, 1981]; i: anorthite rock [*Shelton and Tullis*, 1981]; j: diabase [*Caristan*, 1982]; k: diabase [*Shelton and Tullis*, 1981]; l: diopside rock [*Shelton and Tullis*, 1981]; m: diopside rock [*Kirby and Kronenberg*, 1984]; n: "wet" dunite [*Chopra and Paterson*, 1981].

REFERENCES

Allison, I., and T. E. La Tour, Brittle deformation of hornblende in a mylonite: direct geometrical analogue of ductile deformation by translation gliding, *Can. J. Earth Sci., 14*, 1953-1958, 1977.

Berthé, C., P. Choukroune, and P. Jegouzo, Orthogneiss, mylonite and non-coaxial deformation of granites: the example of the South Armorican Shear Zone, *J. Struct. Geol., 1*, 31-42, 1979.

Birch, F., Compressibility; elastic constants, in *Handbook of Physical Constants*, edited by S.P. Clark, Jr., *Geol. Soc. Am. Mem., 97*, 97-173, 1966.

Biermann, C., (100) deformation twins in naturally deformed amphiboles, *Nature, 292*, 821-823, 1981.

Biermann, C., and H. L. M. Van Roermund, Defect structures in naturally deformed clinoamphiboles—a TEM study, *Tectonophysics, 95*, 267-278, 1983.

Blacic, J. D., Hydrolitic weakening of quartz and olivine, Ph.D. thesis, 205 pp., University of California, Los Angeles, 1971.

Blacic, J. D., and J. M. Christie, Plasticity and hydrolytic weakening of quartz single crystals, *J. Geophys. Res., 89*, 4223-4239, 1984.

Borg, I. Y., Some shock effects in granodiorite to 270 kbars at the Pile Driver Site, *Eos Trans. AGU, 16*, 293-311, 1972.

Borg, I. Y., and Heard, H. C., Further studies on experimentally deformed plagioclase in rock deformation and the deformation mechanisms in torsion tests, *Air Force Cambridge Res. Lab. Rep., AFCRL-67-0308*, 1967.

Borg, I. Y., and Heard, H. C., Mechanical twinning and slip in experimentally deformed plagioclase, *Contrib. Mineral. Petrol., 23*, 128-135, 1969.

Borg, I. Y., and Heard, H. C., Experimental deformation of plagioclases, in *Experimental and Natural Rock Deformation*, pp. 375-403, edited by P. Paulitsch, Springer-Verlag, New York, 1970.

Borges, F. S., and S. H. White, Microstructural and chemical studies of sheared anorthosites, Ronevalm South Harris, *J. Struct. Geol., 2*, 273-280, 1980.

Brodie, K. H., and E. H. Rutter, On the relationships between rock deformation and metamorphism, with special reference to the behavior of basic rocks, in *Metamorphic Reactions: Kinetics, Textures and Deformation*, edited by A. B. Thompson and D. C. Rubie, Advances in Physical Geochemistry, Vol. 4. Springer-Verlag, 1985.

Brown, W. L., and J. Macaudiere, Mechanical twinning of plagioclase in a deformed meta-anorthosite — the production of M-twinning, *Contrib. Mineral. Petrol., 92*, 44-56, 1986.

Buck, P., Verformung von Hornblende-Einkristallen bei Drucken bis 21 kbar, *Contrib. Mineral. Petrol., 28*, 62-71, 1970.

Buck, P., and P. Paulitsch, Experimentalle Verformung von Glimmer und Hornblende Einkristallen, *Naturwissenschaften, 56*, 460, 1969.

Burnham, C. W., Magmas and hydrothermal fluids, in *Geochemistry of Hydrothermal Ore Deposits*, pp. 71-136, edited by H. L. Barnes, New York, John Wiley, 1979.

Burnley, P. C., and S. H. Kirby, Plasticity of clinoamphibole single crystals, *Eos Trans. AGU, 62*, 1030, 1981.

Burnley, P. C., and S. H. Kirby, Pressure-induced embrittlement of polycrystalline tremolite $Ca_2Mg_5Si_8O_{22}(OH,F)_2$, *Eos Trans. AGU, 63*, 1095, 1982.

Caristan, Y., The transition from high temperature creep to fracture in Maryland Diabase, *J. Geophys. Res. 87*, 6781, 1982.

Chao, E. C. T., Shock effects in certain rock-forming minerals, *Science 156*, 192-202, 1967.

Chopra, P. N., and M. S. Paterson, The experimental deformation of dunite. *Tectonophysics 78*, 453-473, 1981.

Cobbold, P. R., and D. Gapais, Slip-system domains. I. Plane-strain kinematics of arrays of coherent bands with twinned fibre orientations, *Tectonophysics 131*, 113-132, 1986.

Dell'Angelo, L. N., and J. Tullis, Experimental deformation of partially melted granitic aggregates, *J. Met. Geol. 6*, 495-515, 1988.

Dell'Angelo, L. N., J. Tullis, and R. A. Yund, Transition from dislocation creep of melt-enhanced diffusion creep in fine-grained granitic aggregates, *Tectonophysics, 139*, 325-332, 1987.

Dollinger, G., and J. D. Blacic, Deformation mechanisms in experimentally and naturally deformed amphiboles, *Earth Planet. Sci. Lett., 26*, 409-416, 1975.

Gavasci, A. T., Investigations on deformation in amphibole and amphibole-bearing xenoliths from the kimberlite-bearing diatremes on the Colorado Plateau, *Air Force Cambridge Res. Lab. Rep., AFCRL-TR-73-0765*, 1973.

George, R. P., and J. M. Christie, Improved sample assemblies for the Griggs solid-medium deformation apparatus, *Eos Trans. AGU, 60*, 371, 1979.

Getting, I. C., and G. C. Kennedy, The effect of pressure on the e.m.f. of chrome-alumel and platinum-platinum 10% rhodium thermocouples, *J. Appl. Phys, 41*, 4552-4561, 1970.

Griggs, D. T., Hydrolitic weakening of quartz and other silicates, *Geophys. J. Roy. Astron. Soc., 14*, 19-31, 1967.

Griggs, D. T., and J. Handin, Observations on fracture and a hypothesis of earthquakes, *Geol. Soc. Am. Mem. 79*, 437-364, 1960.

Hacker, B. R., and J. M. Christie, Unusual submicroscopic defects associated with metamorphic reactions in experimentally deformed amphibolite, *Eos Trans. AGU, 69*, 1417, 1988.

Hansen, F. D., and N. L. Carter, Creep of selected crustal rocks at 1000 MPa, *Eos Trans. AGU, 63*, 437, 1982.

Heard, H. C., Transition from brittle to ductile flow in Solenhofen limestone as a function of temperature, confining pressure and interstitial fluid pressure, *Geol. Soc. Am. Mem., 79*, 193-226, 1960.

Heard, H. C., and W. W. Rubey, Tectonic implications of gypsum dehydration, *Geol. Soc. Am. Bull., 77*, 741-760, 1966.

Ji, S., and D. Mainprice, Natural deformation fabrics of plagioclase: implications for slip systems and seismic anisotropy, *Tectonophysics, 147*, 145-163, 1988.

Ji, S., D. Mainprice, and F. Boudier, Sense of shear in high-temperature movement zones from the fabric asymmetry of plagioclase feldspars, *J. Struct. Geol., 10*, 73-81, 1988.

Jordan, P. G., The deformational behaviour of bimineralic limestone-halite aggregates., *Tectonophysics, 135*, 185-197, 1987.

Kirby, S. H., Localized polymorphic phase transitions in high-pressure faults and applications to the physical mechanism of deep earthquakes, *J. Geophys. Res., 92*, 13789-13800, 1987.

Kirby, S. H., and J. M. Christie, Mechanical twinning in diopside $Ca(Mg,Fe)Si_2O_6$: Structural mechanism and associated crystal defects, *Phys. Chem. Min., 1*, 137-163, 1977.

Kirby, S. H., and A. K. Kronenberg, Deformation of clinopyroxenite: evidence for a transition in flow mechanisms and semi-brittle behavior, *J. Geophys. Res., 89*, 3177-3192, 1984.

Kirby, S. H., and R. W. Lee, Hydroxyl embrittlement of hydrous silicates, *Eos Trans. AGU, 63*, 1095, 1982.

Koch, P. S., Rheology and microstructures of experimentally deformed quartz aggregates. Ph.D. thesis, 464 pp., University of California, Los Angeles, 1983.

Kronenberg, A. K., and G. L. Shelton, Deformation microstructures in experimentally deformed Maryland diabase, *J. Struct. Geol., 2*, 341-353, 1980.

Kronenberg, A. K., and J. A. Tullis, Flow strengths of quartz aggregates: grain size and pressure effects due to hydrolytic weakening, *J. Geophys. Res., 89*, 4281-4297, 1984.

Leake, B. E., Nomenclature of amphiboles, *Can. Min., 16*, 501-520, 1978.

Lee, R. W., and S. H. Kirby, Experimental deformation of topaz crystals: possible embrittlement by intracrystalline water, *J. Geophys. Res., 89*, 4161-4166, 1984.

Lister, G. S., and A. W. Snoke, S-C mylonites, *J. Struct. Geol., 6*, 617-638, 1984.

Luan, F. C., M. S. Paterson, and A. C. McLaren, Synthetic quartz aggregates for deformation studies, *Eos Trans. AGU, 67*, 1207, 1986.

Mao, H. K., and P. M. Bell, Behavior of thermocouples in the single-stage piston-cylinder apparatus, *Carnegie Inst. of Wash. Yr. Bk., 69*, 207-216, 1971.

Marshall, D. B., and A. C. McLaren, Deformation mechanisms in experimentally deformed plagioclase feldspars, *Phys. Chem. Min., 1*, 351-370, 1977a.

Marshall, D. B., and A. C. McLaren, The direct observation and analysis of dislocations in experimentally deformed plagioclase feldspars, *J. Mat. Sci, 12*, 893-903, 1977b.

Montardi, Y., and D. Mainprice, A TEM study of the natural plastic deformation of calcic plagioclase (An 68-70), *Bull. Minéral., 110*, 1-14, 1987.

Morrison-Smith, D. J., Transmission electron microscopy of experimentally deformed hornblende, *Am. Min., 61*, 272-280, 1976.

Murrell, S. A. F., and I. A. H. Ismail, The effect of decomposition of hydrous minerals on the mechanical properties of rocks at high pressures and temperatures, *Tectonophysics, 31*, 207-258, 1976.

Nielsen, K. C., Tectonic setting of the northern Okanagan Valley at Mara Lake, British Columbia, Ph.D. thesis, 150 pp., University of British Columbia, 1978.

Nissen, H.-U., Exsolution phenomena in bytownite plagioclases, in *The Feldspars*, pp. 491-521, edited by W.S. MacKenzie and J. Zussman, Manchester University Press, New York, 1974.

Olsen, A., and D. L. Kohlstedt, Dislocations in some naturally deformed plagioclase feldspars, *Eos Trans. AGU, 62*, 395, 1981.

Olsen, A., and D. L. Kohlstedt, Natural deformation and recrystallization of some intermediate plagioclase feldspars, *Tectonophysics, 111*, 107-131, 1985.

Paterson, M. S., *Experimental Rock Deformation: The Brittle Field*, pp. 254, Springer-Verlag, Berlin, 1978.

Raleigh, C. B., and M. S. Paterson, Experimental deformation of serpentinite and its tectonic implications, *J. Geophys. Res., 70*, 3965-3985, 1965.

Ramsay, J. G., and R. H. Graham, Strain variations in shear belts, *Can. J. Earth Sci., 7*, 786-813, 1970.

Riecker, R. E., and T. P. Rooney, Weakening of dunite by serpentine dehydration, *Science, 152*, 196-198, 1966.

Rooney, T. P., A. T. Gavasci and R. E. Riecker, Mechanical twinning in experimentally and naturally deformed hornblende, *Air Force Cambridge Res. Lab. Environ. Res. Pap., 484* (AFCRL-TR-74-0361), 1974.

Rooney, T. P., and R. E. Riecker, Constant strain-rate deformation of amphibole minerals, *Air Force Cambridge Res. Lab. Environ. Res. Pap., 430* (AFCRL-TR-0045), 1973.

Rooney, T. P., R. E. Riecker and A. T. Gavasci, Hornblende deformation features, *Geology, 3*, 364-366, 1975.

Rutter, E. H., and K. H. Brodie, Experimental "syntectonic" dehydration of serpentinite under conditions of controlled pore water pressure, *J. Geophys. Res., 93*, 4907-4931, 1988.

Seifert, K. E., and A. J. VerPloeg, Deformation characteristics of experimentally deformed Adirondack anorthosite, *Can. J. Earth Sci., 14*, 2706-2717, 1977.

Shelton, G. L., and J. Tullis, Experimental flow laws for crustal rocks, *Eos Trans. AGU, 62*, 396, 1981.

Smith, J. V., *Feldspar Minerals, Vol. 1 and 2*. Springer-Verlag, New York, 1974.

Smith, J. V., Phase relations of plagioclase feldspars, in *Feldspars and Feldspathoids*, pp. 54-94, edited by W. L. Brown, D. Reidel, Dordrecht, 1984.

Tullis, J., Deformation of feldspars. in *Feldspar Mineralogy*, pp. 297-323, edited by P. H. Ribbe, Mineralogical Society of America, 1983.

Tullis, J., and R. A. Yund, Experimental deformation of dry Westerly granite, *J. Geophys. Res., 82*, 5707-5718, 1977.

Tullis, J., and R. A. Yund, Hydrolitic weakening of experimentally deformed Westerly granite and Hale albite rock, *J. Struct. Geol., 2*, 439-451, 1980.

Tullis, J., and R. A. Yund, Dynamic recrystallization of feldspar: A mechanism for ductile shear zone formation, *Geology, 13*, 238-241, 1985.

Tullis, J., and R. A. Yund, Transition from cataclastic flow to dislocation creep of feldspar: Mechanisms and microstructures, *Geology, 15*, 606-609, 1987.

Vernon, R. H., Deformation and recrystallization of a plagioclase grain, *Am. Min., 60*, 884-888, 1975.

Vernon, R. H., V. A. Williams, and W. F. D'Arcy, Grain-size reduction and foliation development in a deformed granite batholith, *Tectonophysics, 92*, 123-146, 1983.

Weertman, J., and J. R. Weertman, *Elementary Dislocation Theory*, 260 pp., Cambridge University Press, Cambridge, 1964.

Wenk, H. R., H. J. Bunge, E. Jansen and J. Pannetier, Preferred orientation of plagioclase—neutron diffraction and U-stage data, *Tectonophysics, 126*, 271-284, 1986.

White, S., Tectonic deformation and recrystallization of oligoclase, *Contrib. Mineral. Petrol., 50*, 287-304, 1975.